NASA Technical Memorandum 106984
AIAA–95–2787

Laser Doppler Velocimeter System for Subsonic Jet Mixer Nozzle Testing at the NASA Lewis Aeroacoustic Propulsion Lab

Gary G. Podboy
Lewis Research Center
Cleveland, Ohio

James E. Bridges
NYMA, Inc.
Brook Park, Ohio

Naseem H. Saiyed and Martin J. Krupar
Lewis Research Center
Cleveland, Ohio

Prepared for the
31st Joint Propulsion Conference and Exhibit
cosponsored by AIAA, ASME, SAE, and ASEE
San Diego, California, July 10–12, 1995

National Aeronautics and
Space Administration

Laser Doppler Velocimeter System for Subsonic Jet Mixer Nozzle Testing at the NASA Lewis Aeroacoustic Propulsion Lab

Gary G. Podboy
National Aeronautics and Space Administration
Lewis Research Center
Cleveland, Ohio 44135

James E. Bridges
NYMA Inc.
Brook Park, Ohio 44142

Naseem H. Saiyed and Martin J. Krupar
National Aeronautics and Space Administration
Lewis Research Center
Cleveland, Ohio 44135

SUMMARY

A laser Doppler velocimeter (LDV) system developed for the Aeroacoustic Propulsion Laboratory (APL) at the NASA Lewis Research Center is described. This system was developed to acquire detailed flow field data which could be used to quantify the effectiveness of internal exhaust gas mixers (IEGMs) and to verify and calibrate computational codes. The LDV was used as an orthogonal, three component system to measure the flow field downstream of the exit of a series of IEGMs and a reference axisymmetric splitter configuration. The LDV system was also used as a one component system to measure the internal axial flow within the nozzle tailpipe downstream of the mixers. These IEGMs were designed for low–bypass ratio turbofan engines. The data were obtained at a simulated low flight speed, high–power operating condition. The optical, seeding, and data acquisition systems of the LDV are described in detail. Sample flow field measurements are provided to illustrate the capabilities of the system at the time of this test, which represented the first use of LDV at the APL. A discussion of planned improvements to the LDV is also included.

INTRODUCTION

In the future it is likely that commercial aircraft will be required to operate at noise levels below the FAR Part 36 Stage 3 requirements of today. Consequently, efforts are underway to develop engine components which will provide an acoustic benefit but will not adversely compromise propulsive efficiency. In particular, as part of NASA's Advanced Subsonic Technology (AST) Noise Reduction Program, Pratt & Whitney and NASA are engaged in a 3 year effort to research, design, and develop internal exhaust gas mixers (IEGMs) which reduce the jet noise of low–bypass ratio (LBR) turbofan engines. The first stage of this task, which is now underway, concentrates on determining a reference level of jet noise corresponding to current technology LBR mixers, and calibrating design codes which will be used to design the next generation of IEGMs.

The design codes include both computational fluid dynamics (CFD) and computational aeroacoustic (CAA) codes. The CFD codes are used to predict the mean and turbulent velocity fields generated by an IEGM at a given operating condition. These flow field predictions serve as input to the CAA codes which then compute an estimate of the noise generated. Detailed flow field measurements are needed to assess the capabilities of the CFD codes, while acoustic measurements are needed to verify the accuracy of the CAA codes. Once these codes are verified and calibrated they can be used to screen potential mixer designs, thereby decreasing the need to carry out expensive and time consuming experimental investigations.

An experiment was recently conducted in the Aeroacoustic Propulsion Laboratory (APL) at the NASA Lewis Research Center to measure the flow field and acoustic properties of three 1/7–scale IEGMs. The configurations tested included a 12–lobe IEGM, a 20–lobe IEGM, and an axisymmetric splitter. The 12–lobe configuration represents a model of the exhaust system of the PW JT8D–200 engine which powers the McDonell Douglas MD–80. The 20–lobe IEGM was designed to provide some acoustic benefit over the baseline 12–lobe configuration. The acoustic data obtained during this experiment serve as a reference for assessing future improvements in noise reduction and as a means of assessing the capability of CAA codes to predict the noise generated by mixer and splitter configurations. The flow field measurements are being used to quantify mixer effectiveness and for the initial calibration of CFD codes. A companion paper presents a comparison between the LDV data and the output of a three–dimensional Navier–Stokes code (ref 1).

This paper describes in detail the LDV system developed for the APL and used to obtain the IEGM flow field measurements. The LDV was used as an orthogonal 3 component system to measure the velocity field at a series of axial stations downstream of the nozzle exit. The system was reconfigured into a one component system to measure the axial velocity at one axial station within the tailpipe of the model. In this paper, the optical, seeding and data acquisition systems of the LDV are described. Sample data are presented to illustrate the capabilities of the LDV system at the time of this test, which represented the first use of LDV at the APL. Possible future improvements to the LDV system are also discussed.

SYMBOLS

x axial distance downstream of nozzle exit

D nozzle exit diameter

r radius

r_o radial extent of nozzle exhaust plume at an axial location

EXPERIMENTAL APPARATUS AND PROCEDURE

Facility and Model Description

This test was conducted at the Aeroacoustic Propulsion Laboratory (APL) at the NASA Lewis Research Center. The APL is a 130 ft. (39.6 m) diameter, acoustically treated, geodesic dome (fig 1). Acoustic wedges on the floor (not shown in fig. 1) and walls render the facility anechoic and reduce the

noise impact on the neighboring communities. The APL houses a free–jet wind tunnel known as the Nozzle Acoustic Test Rig (NATR).

The NATR can simulate low subsonic flight conditions. A set of 30 air ejectors operate simultaneously to pump the required airflow for the free–jet. The ejectors can be supplied with 125 lb/s of compressed air, at 125 psi, to achieve a maximum free–jet airflow of 375 lb/s at Mach 0.3. The centerline of the 53 inch (1.35 m) diameter free–jet is approximately 10 feet (3.05 m) above the floor. During a run the free–jet and nozzle exhaust flows exit the APL through the large side door. A complete description of the NATR is provided by Castner in reference 2.

The test hardware is mounted to the NASA Lewis Jet Exit Rig (JER). The JER, shown schematically in figure 2, is mounted in the duct such that the model and free–jet centerlines are collinear and so that the nozzle exit plane is roughly 2 feet (0.61 m) downstream of the exit of the free–jet tunnel. The JER supplies the test nozzles with core and bypass flows such that high–power operating conditions can be simulated. Air is supplied to the JER through the support strut. The JER contains a flow–through thrust balance, a core flow hydrogen combustor, flow conditioning devices in the core and bypass flows, and pressure and temperature instrumentation. Engine exhaust conditions for the test model are set using this instrumentation.

Figure 3 shows the test hardware installed in the NATR and figure 4 shows a cross–sectional view of the test hardware. The latter figure shows the lobe mixer location and the downstream mixing region. This mixing region is bounded initially on the inside by a plug and on the outside by the convergent nozzle. The design objective of the IEGM is to minimize jet noise from the exhaust flow without incurring significant weight and thrust penalties. Ideally, this is accomplished by rapidly mixing the core and bypass flows within a short mixing chamber.

Three IEGMs, a 12–lobe, a 20–lobe, and an axisymmetric splitter, were tested. During the LDV testing, operating total pressure ratios for the core and bypass were 2.03 and 1.85, respectively. Operating total temperature ratios for the core and bypass were 2.77 and 1.00, respectively. The ratios are referenced with respect to ambient conditions. The free–jet was operated at 0.1 Mach.

LDV System Requirements for the Aeroacoustic Propulsion Laboratory

The LDV test requirements were to obtain a set of highly accurate, highly detailed flow field data for calibrating CFD design codes. The output of these CFD codes is used as input to CAA codes, which then estimate the noise produced from a nozzle operating at a specified condition. The key flow field features of interest are the shear layers at the interface between the primary and secondary flow streams, and the shear layers between the nozzle exhaust jet and the free–jet flow. Noise is created in these shear layers and it is necessary for the CFD codes to accurately predict the mean velocity gradients and the turbulence intensities within these layers in order for the CAA codes to accurately predict the acoustics. Therefore, the data requirements for the LDV testing were 1) to accurately resolve the shear layers in terms of mean velocity fields, 2) define how rapidly the core and bypass flows mix–out, and 3) provide quantitative turbulence intensity levels within the exhaust duct and the near–field jet.

Given the data requirements, the following were considered in the development of the LDV system:

1) The nozzle exhaust flow was expected to be at a very high velocity. Preliminary CFD calculations

indicated that in the case of the reference splitter configuration, where the mixing between the core and bypass flows is relatively limited, velocities approaching 1900 ft/sec (579 m/sec) could be expected. The LDV system optics and signal processing electronics would have to be chosen such that this high velocity could be measured.

2) High flow accelerations would occur. The highest accelerations were expected just downstream of the nozzle exit, where the exhaust flow expands to ambient pressure. The LDV seed material would have to be small enough to follow the flow accelerations with negligible lag. The LDV system receiving optics would have to be able to "see" these small particles.

3) The flow exiting the mixer could be thought of as circumferentially periodic but not axisymmetric. Therefore it would be necessary to map the flow within a pie–slice shaped sector extending circumferentially over at least one half of a lobe.

4) The LDV laser and optical components would have to be located outside the jet flow created by the 53 inch (1.35 m) diameter NATR. Otherwise, the impingement of the flow might vibrate the laser and/or misalign the LDV system optics. Vibration could misalign the mirrors within the laser resulting in a decrease in laser beam power.

5) Three separate flows – the nozzle core, the nozzle bypass, and the free–jet – are being mixed within the nozzle exhaust plume. In order for the LDV to accurately measure the time–averaged, mean velocity flow field within the plume, it would be necessary to seed each of these flows separately.

6) To simulate actual turbofan engine operating conditions, the primary flow would be heated to a total temperature of 1440 deg Rankine during the LDV testing. A solid seed material with a melting point above this operating temperature would be required.

The above considerations led to the development of an orthogonal, three component, forward–scatter LDV system. This system is described in the following sections.

Traverse System

The description by Patrick & Patterson (ref 3) of a previous LDV investigation of a forced mixer ejector nozzle provided some insight regarding the desired LDV system configuration. In their paper, the authors emphasize the need to use particles less than one micron in diameter to ensure that the seed follows the flow with negligible lag. They also explain that for an LDV system to generate adequate signals off of these submicron particles, it is best to place the receiving optics so that they collect the light scattered by the particles in the "forward" direction (i.e. place the receiving optics on the side of the probe volume opposite that of the lens used to cross the laser beams). This forward scatter arrangement is preferred since the submicron seed particles scatter light much more effectively in the forward direction. A major difficulty in employing a forward scatter arrangement involves the requirement that the receiving optics remain focused on the probe volume as the probe volume is moved to different locations in the flow field. Thus, it is necessary to move the receiving optics the same distance and in the same direction as the transmitting optics. The most reliable means of doing this is to traverse both sets of optics in unison using a single traversing system. In the APL, since the optics must be outside the shear layer created by the 53 inch (1.35 m) diameter NATR, a large scan rig is required.

A photograph of the scan rig developed for the APL is shown in figure 5. This scan rig was modeled after a number of similar systems developed at NASA Langley for laser velocimeter testing. The basic "building blocks" of the rig are commercially–available, extruded–aluminum rails. These are fastened together to form a 98 X 98 X 60 inch (2.49 X 2.49 X 1.52 m) inner "cube" on which the laser and optics are mounted. During a run, the nozzle and free–jet flows pass through the two square sides of this inner cube. This cube was sized so that it would be outside the shear layer of the free–jet at all times, thus avoiding any flow–induced vibration of the LDV system optics. When positioned to acquire data at the nozzle centerline, the top of the inner cube is roughly 14 feet (4.27 m) above the APL floor. Four motorized slides are used to translate the inner cube in the vertical direction. This cube is mounted to an outer cube which is translated horizontally in the lateral (cross stream) and longitudinal (axial flow) directions using eight other slides. One meter (3.28 ft) of travel in each of the three directions is provided with 10 micron (0.00039 in) resolution. The scan rig is remotely controlled via an RS232 link with the MicroVAX 3400 LDV system computer.

Three Component Optical Setup

When the LDV system was configured to measure three velocity components, optics were mounted on four separate breadboards attached to the inner cube. A schematic showing the placement of these four breadboards on the scan rig is shown in figure 6. Breadboards 1 and 2 hold transmitting optics which direct laser beams into the flow, while breadboards 3 and 4 carry receiving optics which collect light scattered from particles passing through the probe (measurement) volume. Flow field velocities are measured by determining the fringe–crossing frequency of seed particles embedded in the flow field as they traverse the interference pattern (fringes) created at the intersection point (probe volume) of two laser beams of like color. With the three component optical configuration, three separate probe volumes are created using pairs of green, blue and violet laser beams. Photomultiplier tubes convert light scattered from a particle passing through a probe volume into an electrical signal (Doppler burst), the frequency of which is equivalent to the fringe–crossing frequency. The spacing of the fringes of the interference pattern is a known function of the crossing angle formed by the two intersecting laser beams and the wavelength of the laser light. The particle velocity component lying in the plane of the two laser beams, and perpendicular to the bisector of the two beams, is computed by multiplying the fringe spacing by the fringe–crossing frequency.

The 4 X 5 ft. (1.22 X 1.52 m) breadboard labeled #1 in figure 6 is mounted at the bottom of the inner cube alongside an Argon ion laser. The laser emits a single beam of light containing a number of wavelengths within the visible spectrum including 476 nm (violet), 488 nm (blue) and 514.5 nm (green). The layout of the optics on breadboard #1 is shown in figure 7a. A mirror is used to direct the multicolored laser beam onto the breadboard where it passes through a beam collimator and a polarization rotator before entering a TSI model 9201 color separator. A single Bragg cell within the color separator is used to split the input beam into its different wavelengths such that two beams of each wavelength are generated. One of the two beams of each wavelength is frequency shifted 40 MHz by the Bragg cell. A series of prisms and mirrors are used to direct two green (514.5 nm wavelength), two blue (488 nm) and two violet (476 nm) beams out of the color separator.

In the three component setup, the two green and two blue beams were used to measure the axial and vertical velocity components, respectively. In this configuration, the green and blue beams are passed through a set of alignment prisms and a set of 13 mm (0.51 in) beam spacers before being directed by mirrors up to breadboard #2, which is mounted off the side of the inner cube. On this 2 X 4 ft. (0.61 X 1.52 m) breadboard, the beams pass through a 3.75 X beam expander and a 1200 mm (3.94 ft) focal

length focusing lens (see figure 7b). Each set of colored beams then cross, creating a probe volume at their intersection point. The alignment prisms are used to force the green and blue probe volumes to overlap.

Green and blue laser light scattered in the forward direction from particles passing through the probe volume is collected by the receiving optics mounted on breadboard #3 of figure 6. Separate sets of receiving hardware are provided for each of the two components (see figure 7c). Each set consists of a six inch (0.152 m) diameter "collecting" lens, a six inch diameter "focusing" lens, a remotely–controlled turning mirror, a color filter, a pinhole, and a photomultiplier tube. The 1500 mm (4.92 ft) focal length collecting lens collects the light scattered from the particles passing through the probe volume, while the focusing lens (450 mm (1.48 ft) focal length) focuses this light onto a turning mirror which directs it through a pinhole and onto the detector of the photomultiplier tube. The turning mirror is mounted on two remotely–controlled rotary stages which can be used to fine–tune the alignment of the probe volume image with the pinhole to maximize the signal–to–noise ratio of the Doppler bursts. The only difference between the two sets of receiving hardware mounted on breadboard #3 are the color filters inserted in front of the photomultiplier tubes. One filter passes green light, while the other passes blue. Thus it is possible to separate the axial velocity (green) signals from those of the vertical (blue) component.

To measure the third (cross–stream) component of velocity, optics mounted to breadboard #1 are used to direct two violet beams into the flow from below the free–jet. This vertical beam path is orthogonal to the horizontal optical path of the green and blue beams. These violet beams pass through alignment prisms, a 22 mm (0.87 in) beam spacer, a 3.75 X beam expander and a 1500 mm (4.92 ft) focal length focusing lens. An eight inch (0.203 m) mirror reflects the beams upward into the flow. Tilt and pan adjustments on the mirror mount are used to overlap the probe volume created by the violet beams with those of the green and blue beams.

Receiving optics mounted on breadboard #4 of figure 6, at the top of the scan rig, are used to generate the Doppler signals for this third component. The layout of these optics is shown in figure 7d. Except for the color filter, this receiving hardware is identical to that used for the other two components. Here, a narrow band pass color filter centered about the 476 nm wavelength of the violet beams is used. This filter selectively passes the cross–stream velocity signals, and discards the others.

Aligning the receiving optics located on this breadboard, some 14 feet (4.27 m) above the floor, proved difficult. This breadboard was mounted vertically to allow a direct path of the scattered light into the collecting lens. Consequently, it was necessary to hold onto a component as it was being aligned to keep it from falling. Once alinged, that item was clamped into place, and the alignment was continued with the next piece. This was repeated until all the receiving hardware was aligned. To mount these items it was necessary to add some extra aluminum rails across the inner cube of the scan rig. These rails were used to stand on and lean against while the pieces were being mounted. It became apparent that the weight of the people standing on these rails flexed the inner cube to the point that the optical alignment of the receiving hardware with the probe volume changed once the people came down off the scan rig. Fortunately, it was possible to use the two rotary stages on which the turning mirror was mounted to remotely re–align the system. The mirror was rotated until the probe volume image once again passed through the pinhole in front of the photomultiplier. This was accomplished by flowing a seeded, low velocity jet through the probe volume and observing the output signal from the photomultiplier on an oscilloscope. Alignment was achieved when the signal–to–noise ratio of the Doppler bursts was maximized.

Table 1 provides an estimate of the size of each of the three probe volumes resulting from the optical configuration described above. Two sizes are shown for each of three probe volumes – one is listed as the "on–axis" size and the other as the "off–axis" size. The "on–axis" size corresponds to the actual size of the ellipsoid created by the intersecting laser beams, while the "off–axis" size is the size of the probe volume "visible" to the photomultiplier tube used to measure a particular component. The on–axis sizes, listed at the left in the table, were computed based on the characteristics of the laser beams and the transmitting optics. These sizes are a function of the laser beam wavelength, the laser beam diameter, the beam spacing, the beam expander magnification, and the focal length of the focusing lens. These numbers would correspond to the actual sizes of the probe volumes "seen" by the photomultipliers if the receiving optics were mounted "on–axis" (i.e in–line) with the transmitted laser beams. Placing the receiving optics "off–axis", however, in combination with the use of a spatial filter (pinhole), effectively shortens the probe volume length. The length decreases as the angle between the laser beams and the collection lens increases, and reaches a minimum at an angle of 90 degrees. In the three component optical arrangement, the off–axis angles were approximately 30, 15 and, 15 degrees for the green, blue and violet collecting lenses, respectively. These result in the probe volume dimensions listed at the right in the table.

One Component Optical Setup

In order to obtain velocity measurements within the nozzle tailpipe it was necessary to reconfigure the optical setup from that described above. For the internal measurements, windows were required to allow optical access to the flow. To allow a forward scatter optical system, two windows were required; one to allow the transmitted beams into the tailpipe, and one to allow the forward–scattered light out to the receiving optics. To provide this access, two flat, one inch (25.4 mm) diameter, 5/16ths inch (7.9 mm) thick, quartz windows were mounted in the tailpipe. These were located axially just downstream of the plug and circumferentially at the three and nine o'clock positions. This arrangement allowed the optics mounted on the two side breadboards to be used to measure the internal axial velocities. These small diameter windows did not permit an off–axis arrangement of the receiving optics. Instead, these optics had to be moved in–line with the laser beams in order for the collecting lens to be able to view the probe volume. This configuration is shown in figure 8. Only one collecting lens could be positioned to view the probe volume through the window. Therefore, only one component of velocity, the axial component, was measured.

If the internal flow was circumferentially periodic lobe–to–lobe, it would only be necessary to acquire data within a pie–slice shaped sector extending over one–half of a primary lobe and one–half of a secondary lobe. To check this periodicity it was decided to obtain data over a minimum of one complete primary lobe, extending circumferentially from one lobe trough to another. The small access windows, however, did not allow a sector of this size to be viewed completely. Consequently it was necessary to obtain the desired internal data over the span of two runs. In the first run, the pie–slice shaped sector was mapped as completely as possible given the optical constraints. Then the rig was shut down and the mixer was physically rotated by 9 degrees to allow access to the previously hidden measurement locations. Data were then acquired to complete the desired matrix.

Laser Vibration

As discussed in the preceding sections, the scan rig was sized so that the laser and optics would be just outside the free–jet shear layer. Nevertheless, with the free–jet operating at 0.3 Mach the flow

caused the laser to vibrate to the point that its power output was reduced to unacceptable levels. The vibration is thought to have resulted from having the large 4 X 5 ft. (1.22 X 1.52 m) breadboard too close to the free–jet flow. The pressure fluctuations within the shear layer acted on this large "flat plate", resulting in vibration of the entire scan rig. In order to reduce the vibration, it was necessary to run the free–jet at 0.1 Mach. As an added measure, the 15 watt laser used at the beginning of the test was replaced with a smaller 6 watt laser. This smaller laser was less susceptible to vibration.

Seeding

There were two requirements for the LDV seeding material. One, it had to have a melting point temperature above the 1440 deg Rankine stagnation temperature of the core flow; and, two, it had to be in the size range of about 0.5 to 1.0 micron. This size range is preferred since these particles would be small enough to follow the flow, yet big enough to generate adequate Doppler signals. There are a number of metal oxide powders which are sold as satisfying these criteria, including alumina and titanium dioxide.

Unfortunately, even though product specifications may indicate that a powder is commercially available within a desired size range, interparticle forces cause the particles to agglomerate to the point that when they arrive from the manufacturer, most of the particles are too big to adequately follow a rapidly accelerating flow. In practice, this represents a major difficulty since it is necessary to break up the agglomerates and/or selectively separate out and discard the bigger particles. Normally, in LDV applications using metal oxide powders, fluidized beds are used to generate the dry aerosol needed to seed the flow. In this case, it is necessary to create a flow within the bed which can shear apart the agglomerates. In addition, cyclone separators can be used to separate out the larger particles.

Previous experience in an LDV test of a High Speed Research (HSR) nozzle revealed that it can be difficult to operate a fluidized bed to obtain a continuous output of seed. After turning on the nitrogen supply to this fluidized bed, acceptable levels of output were sustained for only about ten seconds. After this short period of time, very little powder was being fluidized; evidently, due to a lack of powder within the paths of the internal jets used to fluidize the seed material. Consequently, it was necessary to cycle the fluidized bed on and off. Apparently, during the off periods the powder settled back into the paths of the internal jets. Unfortunately, the bed had to sit idle for about a minute in order for enough of this settling to occur to achieve a reasonable output once the supply was turned back on. Therefore, before this fluidized bed could be used in another test, it would be necessary to provide some means of continuously mixing seed into the paths of the internal fluidizing jets.

For the LDV test in the APL, rather than modify the fluidized bed, it was decided to use a method of seeding with metal oxide particles recently described in a paper by Wernet and Wernet (ref. 4). With this method, rather than using a dry powder, the metal oxide is suspended in a liquid. While in solution the agglomerated particles are broken apart using a sonicator and/or a laboratory blender. The surface charge on the particles is controlled by adjusting the pH of the solution. The pH is adjusted so that like charges build up on the surface of the particles. These like charges cause the particles to repel one another and, therefore, prevent the particles from flocculating. This stable dispersion of particles in solution can then be sprayed into the flow. The evaporation of the liquid droplets leaves behind a dry aerosol of seed particles of the desired size. By continuously spraying the solution into the flow, a continuous supply of seed particles is maintained.

In this test, alumina seed particles were introduced into three separate flows – the primary model flow, the secondary model flow, and the external free–jet. The alumina particles were relatively monodisperse with a mean diameter of 0.7 micron and a standard deviation of 0.2 micron. Two different seed solutions were created – a 5% by weight alumina in water solution for the internal model flows and a 1% by weight alumina in water solution for the free–jet.

The 5% solution was atomized by a set of four TSI Inc. six–jet atomizers. Two six–jet atomizers supplied seed to the primary flow, and two supplied the secondary. Each six–jet unit atomized approximately six ounces of solution per hour. The seed was introduced into the model via a seeding "rake" in each of the primary and secondary flow streams. The seeding rakes were mounted in a cylindrical spool piece located 50 inches (1.27 m) upstream of the nozzle exit. A photograph of the spool piece with the seeding rakes installed is shown in figure 9. The axial position of this rake relative to the nozzle hardware is illustrated in figure 10. These rakes were mounted horizontally in the spool piece at the 3 o'clock position. The atomized seed solution flowed through ten output ports in the primary rake and six in the secondary. These holes were sized so that with the atomizers set 5 psi above the internal model pressures, the velocity of the individual seeding jets would be roughly the same as the velocity of the streams into which they were flowing. Also, the mass flow output by the two seeding rakes would be a small fraction of the total mass flow within the model. As such, the seed injection would have little effect on the downstream flow which was to be measured.

The high core temperature ensured that the atomized liquid droplets introduced into the primary would evaporate before reaching the mixer exhaust region where the LDV measurements were made. To ensure that the droplets injected into the secondary flow also evaporated, the air supply to the secondary was dried. This drying, in combination with the mixing of the hot core flow, allowed the small mass of liquid added by the atomizers to evaporate. This was checked by introducing atomized droplets of water (minus the alumina particles) into the flow and monitoring the data rate. A very low data rate indicated that the liquid was indeed evaporating. Under normal testing conditions, with alumina seed added to the water, data rates were typically between 500 and 1000 samples/sec.

The 1% alumina solution was sprayed into the free–jet flow using a spray nozzle developed for icing tests in the NASA Lewis Icing Research Tunnel. The nozzle used was of the "mod–1" type as described in a paper by Ide (ref 5). This is an air–assist atomization nozzle which was operated to deliver approximately one gallon of solution per hour into the free–jet flow. The nozzle was attached at the free–jet centerline to the honeycomb in the bellmouth of the NATR. This placed the nozzle 22.5 feet (6.86 m) upstream of the NATR exit plane. This one nozzle provided seed densities such that data rates of up to 800 samples/sec were realized in the free–jet flow outside the mixer nozzle exhaust plume.

Data Acquisition System

The Doppler signals detected by the LDV system receiving optics were converted to analog electrical signals by the photomultiplier tubes and transferred to signal processing hardware located in a trailer outside the APL which served as the control room for the LDV testing. The signals were carried approximately 120 feet (36.6 m) through coaxial cables to Macrodyne, Inc. model 3107 Frequency Domain Processors (FDP). A separate signal processor was used for each of the three velocity components. These processors digitize the incoming analog Doppler signals with an 8 bit A/D converter and then compute the Doppler frequency using a Fast Fourier Transform. With these units the digitizer sampling frequency could be set as high as 300 MHz, allowing the measurement of Doppler

signals up to 120 MHz. With a fringe spacing of nominally 13 microns, a maximum axial velocity of 1900 ft/sec (580 m/sec), and a 40 MHz frequency shift in the opposite direction to the mean axial flow, the maximum expected Doppler frequency was roughly 85 MHz – well within the capabilities of signal processor.

The 3107 FDP was recently tested by Hepner (ref 6) as part of a study to determine the relative accuracy of seven different commercially–available LDV signal processors. The processors were tested over a frequency range of 2 to 49.9 MHz using synthesized signals similar in amplitude, duration, and quality (signal–to–noise ratio) to those which might be measured during an actual LDV test. At each 0.1 MHz step within the 2 to 49.9 MHz range, an ensemble of 100 synthesized Doppler waveforms were fed into the signal processors. The standard deviation about the mean frequency within each ensemble was very small, with the variation in frequency about the mean of only +/–1 Hz. With such a narrow distribution of frequencies, any scatter about the mean in the measurements would be an artifact of the signal processors themselves. Consequently, this provides a good test of the ability of a signal processor to measure a small standard deviation, which in a real flow would correspond to a low turbulent velocity. For each ensemble, a mean and standard deviation was computed from the measured frequencies of each signal processor, and these were then compared to the known true values. The 3107 FDP was found to provide estimates of the mean which were within 0.1% of the true values over the tested frequency range for input signals having a signal–to–noise ratio of 24 to 30 dBm. For an ensemble of 30 dBm signals centered about 49 MHz, the 3107 showed an order of magnitude improvement in measuring the ensemble's small standard deviation when compared to the older Macrodyne 3000 series counter processors. The data from this study indicate that the 3107 FDP is capable of accurately measuring standard deviations which are smaller than those which would be provided by the level of turbulence encountered in the nozzle testing in the APL.

During the nozzle test, after being validated by the signal processors, the measured frequencies were transferred to a buffer interface and then into a MicroVAX 3400 computer. Besides providing a temporary storage area for the data, the buffer interface also measured the time interval between successive data points on each velocity channel. During the runs in which the LDV system was configured to measure all three velocity components, the data were acquired in "random" mode, meaning that the three signal processors acquired data independently. This "random" mode of acquisition allows the measurement of the normal components of the Reynolds stress, but not the cross terms. To measure the cross terms it would have been necessary to acquire the data in "coincidence" mode. In coincidence mode the data are kept only when all three signal processors acquire data simultaneously (within a very short time window) on a particle. This coincidence requirement, however, tends to greatly reduce the rate at which data are acquired. Consequently, this requirement was not invoked.

The buffer interface was programmed to accept data from all three channels until one of the processors had obtained a preset number of measurements. Normally during this test, data were acquired until one of the processors had obtained 12000 measurements. On–line data plots of the histograms of the measured frequencies indicated that a sufficient number of measurements were obtained to accurately resolve the mean and turbulent flow velocities for all three velocity components. Typically it took 15 to 20 seconds to acquire the data at each measurement location and another 30 to 40 seconds to process the data on–line, plot it in histogram form, and move the probe volume to the next measurement location. Approximately 50 measurements were made within an axial plane to map the flow within a pie–slice shaped sector spanning a complete lobe. During a run, once a complete set of data were acquired at a given axial location, the data could be transferred to a workstation on which the mean velocities could be displayed as color contours.

Data Post Processing

Post–test data processing consisted primarily of two functions: 1) discarding outliers in the velocity histograms and 2) correcting for velocity bias. As explained by Hepner in his evaluation of LDV signal processors (ref 6), the new processors which employ frequency domain techniques such as the 3107 FDP provide better signal detection, noise rejection, and improved accuracy relative to the older counter processors. Nevertheless, these new processors will output spurious data points when allowed to trigger on noise. In the nozzle test data, there were some histograms which showed measurements which were obviously not generated by particles passing through the probe volume. An example of such a histogram plot is shown in figure 11. In many cases, when bad data were recognized in the on–line histogram plots, the trigger level and/or the filter bandwidth of the signal processor were adjusted to reject these data and then the data point was repeated. As an added measure to ensure that all such bad data were eliminated, each histogram was replotted after the test, and the outliers were discarded as needed.

Velocity biasing was recognized as a potential problem since the flow in the nozzle exhaust plume results from the mixing of three separate flows – the nozzle core (primary), the nozzle bypass (secondary), and the free–jet. Velocity biasing occurs whenever there is a correlation between data rate and velocity. For example, suppose a high velocity stream was mixing with a low velocity stream such that the velocity at a point in space oscillated between the high and low values. If the high velocity stream was seeded but the low velocity stream was not, then the mean velocity calculated from measurements made at that point would most likely be biased high relative to the true time–averaged velocity occurring at that location. In application, it is necessary to seed the different flow streams in such a way that velocity biasing does not occur, or to correct for it in the data reduction.

In this test, the three different flow streams were seeded in an effort to eliminate velocity biasing. Nevertheless, the data were corrected using a velocity bias correction method developed by Meyers and Edwards (ref 7). This method attempts to compute a true time–average of the measurements by dividing the time history of the measured flow into equal time increments. The time increment is chosen based on an integral time scale of the flow estimated from the LDV velocity measurements. Only the first data point within each time increment is then used to calculate the measurement statistics. This method approximates even–time–sampling, and therefore, the computed mean value would be expected to be close to the true time–average.

The results of applying the correction scheme to the data indicate that little, if any, velocity biasing was encountered. This is illustrated in figure 12, which shows a comparison of data before and after applying the correction. The dotted and dashed lines represent uncorrected and corrected data, respectively. The distributions show axial velocities obtained from a radial traverse of the probe volume through the nozzle exhaust plume at an axial location four nozzle diameters downstream of the nozzle exit plane. This data was acquired with the axisymmetric splitter nozzle. As can be seen from the figure, the two distributions practically overlap, indicating that the corrections to this data were very small. This was found to be the case for all of the data obtained during the test. The corrections for velocity bias were typically on the order of 0.2 ft/sec.

RESULTS AND DISCUSSION

Sample Results

Figure 13 is provided to illustrate the density of a typical measurement grid employed during the test. Normally data were acquired at 49 measurement locations per lobe. The circumferential and radial extent of the measurement sector depended on the mixer nozzle being tested and the axial location at which measurements were being made. As a minimum, it was intended to acquire data over a sector extending circumferentially from one primary lobe trough to another, and radially out from the nozzle centerline to a radius ratio, r/r_o, of 0.96. The value of r_o varied depending on axial location. For the internal data, r_o was the local internal radius of the exhaust duct. For the external data, r_o corresponded to the nozzle radius at the nozzle exit plane, and increased with axial distance downstream to account for the estimated 5^o expansion of the nozzle exhaust jet. The measurement locations depicted in figure 13 correspond to the grid density used to map the flow downstream of the 20–lobe mixer. The spacing of the measurement locations within the sector was chosen so that the locations would be roughly at the center of equal area cells.

Figure 14 shows an example of data obtained inside the nozzle tailpipe. The schematic shown near the top of the figure shows the axial location at which these measurements were made relative to the nozzle hardware. Normalized axial velocities measured within the sector are plotted as color contours. These data were normalized by subtracting off from the local axial velocity the axial velocity measured at the nozzle centerline within this plane. So rather than absolute axial velocity, the contours represent the axial velocity difference relative to the value measured at the centerline. These data and the data of the following figures were acquired during testing of the 20–lobe mixer. The view depicted is from downstream looking upstream at the flow occurring at this axial station. The outlines of three of the 20 lobes and the duct radius at the mixer exit are shown superimposed on the color contours. The duct radius is shown to illustrate the gap between the lobes and the duct wall. Also shown is the outline of the flat, one–inch diameter window which permitted optical access to the flow. The window is located radially inboard of the duct radius at the mixer exit. This is due to the convergence of the nozzle tailpipe. In this figure, the inner portions of the "island" of high velocity flow exiting the primary lobe can be seen. Note, however, that data are not plotted for the outermost radial locations within the sector. Data could not be obtained at these outer radial locations because of reflections of the laser beams off the window. As explained previously, to acquire the internal data the receiving optics were placed "on–axis" (i.e. in line with the laser beams). Therefore, the reflections off the window were in the field of view of the receiving optics. The reflections decreased the signal–to–noise ratio to the point that the Doppler signal frequencies could not be measured by the signal processors.

Figure 15 shows axial velocities measured 0.25 inches downstream of the nozzle exit. These velocities have been normalized by subtracting off the axial velocity measured at the nozzle centerline. In this figure data are shown plotted over two of the 20 lobes. The flow across two lobes was mapped to determine the degree of flow periodicity lobe–to–lobe. As can be seen from the figure the axial flow appears to be quite periodic downstream of the mixer lobes. The flow does, however, seem to be rather nonaxisymmetric near the nozzle centerline. Also illustrated by the contours is the merging together of the discreet "islands" of high velocity depicted previously in the internal data of figure 14.

Figures 16 and 17 illustrate the downstream development of the nozzle exhaust plume. Figure 16 shows normalized axial velocities measured at x/D=1, while figure 17 shows data acquired at x/D=2. Once again, the data were normalized by subtracting off the respective centerline axial velocities measured within each axial plane. The x/D=1 data extends out to a radius ratio, r/r_o, of only 0.70. This dataset was not completed due to a mechanical problem with the scan rig. The contours indicate, however, that data were acquired beyond the outer edge of the high velocity region set up by the primary lobes. These data show that by one nozzle diameter downstream of the nozzle exit, the primary and secondary flows have mixed to the point that it is difficult to identify the flows set up by the individual lobes. The once discreet "islands" have merged to form an annular ring of high velocity. By the time the flow reaches x/D=2 (figure 17), the flow has developed to the point that the exhaust plume is relatively uniform out to the nozzle exhaust/free–jet shear layer. In the shear layer the mean axial velocities drop off rapidly as indicated by the closely spaced color contours encircling the core of the jet.

The data obtained in this test indicate that as the scan rig was traversed axially away from the nozzle exit plane, the apex of the measurement sector was displaced further and further from the nozzle jet centerline. This was suggested in the downstream data by the color contour "circles" plotted in the nozzle exhaust/free–jet shear layer. As illustrated in figure 17, radius R1 is less than R2. If the apex of the measurement sector was at the centerline, R1 would be expected to equal R2. Further downstream, at x/D=4 (not shown), this displacement between the apex and the centerline was even larger. This suggests that either the model or the scan rig was not level. Since the scan rig was leveled using a theodolite, it is suspected that the model was pointing down slightly. This model "droop" was also indicated by the vertical velocity components measured at the centerline at the nozzle exit. Due to flow symmetry about the centerline, it would be expected to measure a zero vertical velocity at this point. Normally, however, the measured values were on the order of –40 ft/sec. The negative value suggests that the model was pointing downward. A rough estimate based on the LDV data is that the model was pitched down about one degree. This is not a big problem for the axial velocities since at the downstream stations where the displacement is larger the jet core axial velocity profile is relatively flat. It does, however, make it difficult to create meaningful plots of the secondary velocities occurring within a plane. These secondary velocities were relatively small in comparison to the axial flow. The bias due to the nozzle droop was roughly of the same magnitude as the variation of the secondary velocities within a plane.

The axial velocities shown in the preceding plots were normalized to prohibit comparisons of absolute axial velocities measured at different times during the test. This was done since, in general, it was difficult to get good repeatability of the measured axial velocities. It was not uncommon to find axial velocity variations of 100 ft/sec between data acquired at what was thought to be the same physical location within the flow but on different days. In fact, it was noted that the centerline axial velocity measured at the nozzle exit varied by about 100 ft/sec over the span of a five hour run. The exact cause of these variations is not known. However, a subsequent LDV test of a High Speed Research (HSR) model in the APL revealed that the strut–mounted HSR model moved in both the horizontal and vertical directions during a run. It is possible that the IEGM model for which LDV data is presented in this paper also moved. This movement of the model could account for the poor data repeatability. Since these variations did occur it was decided that the data acquired within each plane would be normalized by subtracting off the centerline axial velocity.

Figure 18 is presented to illustrate that after the data is normalized in this manner, the repeatability is quite good. Presented in this figure are the normalized axial velocity data obtained on two different days. The main difference between the two plots is the thickness of the low velocity (blue) region near the outermost edge of the contours. This difference may have been caused by a sideways movement of the model during the course of a run. Inaccuracies in locating the probe volume relative to the nozzle hardware may also account for this difference. As part of each days pre–run setup, an attempt was made to locate the origin of the scan rig coordinates at the nozzle exit centerline. In the vertical direction this was relatively easy. It was simply a matter of determining how far the scan rig had to translate in order to move the probe volume from the lowest point of the nozzle lip to the highest point, move the probe volume back one–half this distance, and "zero" the vertical direction readout. In the horizontal (transverse) direction, this was made more difficult because of the long length of the probe volume. Thus it was difficult to locate the exact center point of the probe volume relative to the nozzle lip. Consequently, discrepancies could have occurred between the day–to–day setting of the origin of the scan rig coordinates relative to the model. The data of figure 18 indicate that the origin on 9/18/94 may have been displaced slightly to the right relative to the origin of 7/29/94.

Figure 19 shows contours of axial turbulence intensity computed from the measurements made just downstream of the nozzle exit at x=0.25 inch. The axial turbulence intensity is defined as the local turbulent axial velocity divided by the local mean axial velocity. The turbulent velocity is computed from the LDV data as the standard deviation of the velocities measured at a location. The standard deviation can be thought of as a measure of the width of a velocity histogram (fig. 11) . In figure 19 the turbulence intensities are shown as a percentage by multiplying the computed velocity ratios by 100. The previously presented axial velocity contours for this axial station are shown replotted at the bottom of figure 19. As can be seen in the figure, the axial turbulence intensity is relatively uniform out to a radius ratio of about 0.70. This corresponds to a radial location close to where the maximum axial velocities were measured. Further outboard, as the velocity gradient increases, the turbulence intensity also increases, reaching levels of almost 12%. These data were obtained inboard of the region in the flow having the highest velocity gradient – the nozzle plume/free–jet shear layer. In the shear layer the axial turbulence intensities would be expected to increase dramatically.

If the model was moving during the acquisition of the LDV data, it is likely that the measured axial turbulence intensities would be biased high relative to what they would have been if the model was stationary. This bias would be caused by a change in the mean flow passing through the probe volume over time. This change in the mean flow would broaden the measured velocity histogram, resulting in a higher computed standard deviation, and hence, a higher turbulent velocity. For this bias to be significant, the mean flow would have to change appreciably within the amount of time required to obtain the data at a given measurement location. It should be pointed out, however, that this bias could be expected to be small if the movement of this model was similar to that of the HSR model. While it typically took only between 15 and 20 seconds to acquire data at a given point in the flow field, the period of oscillation of the HSR model was on the order of several minutes. Consequently, the model would move only slightly over a data acquisition period, and the histogram broadening due to mean flow changes would be expected to be slight.

Concluding Remarks and Recommendations

This paper was intended to describe the capabilities of the LDV system developed for the Aeroacoustic Propulsion Laboratory at the NASA Lewis Research Center. In this first LDV test at the APL, it was demonstrated that the LDV system is capable of obtaining data of sufficient accuracy and detail to guide

the calibration of CFD design codes. The following suggestions might help increase the system capability:

1) Determine why it was not always possible to get good data repeatability. As suggested by the subsequent HSR model LDV testing, the variations noted in the axial velocity measurements made at a given location may have been caused by the movement of the model over the course of a run. If this is the case, it is necessary to either prevent or measure and account for any such movement.

2) Make the centerline of the nozzle flow parallel to the downstream traverse direction of the scan rig. That is, eliminate any downward and/or sideways "pointing" of the model. This can be accomplished by repositioning the model, the scan rig or both.

3) Make it possible to acquire internal data closer to the window. This might be possible by repositioning the receiving optics "off–axis". By positioning the receiving optics so that they "look" into the flow through the nozzle exit opening it might be possible to reduce the amount of flare "seen" by the photomultiplier. This would increase the signal–to–noise ratio of the Doppler signals, making it more likely that they would be measured by the signal processors.

4) Make the laser and optics less susceptible to vibration so that data can be acquired with the free–jet operating at higher Mach numbers. This can be achieved by moving the laser and the 4 ft. X 5 ft. (1.22 X 1.52 m) breadboard mounted at the bottom of the inner cube further away from the free–jet flow. This would be possible by increasing the height of the inner cube through the use of longer vertical aluminum rails. This would allow the other three breadboards to remain at the same positions while moving the laser and the 4 ft. by 5 ft. (1.22 X 1.52 m) breadboard further below the free–jet.

REFERENCES

1. Zysman, S.H., Saiyed, N., Podboy, G.G., Chiappetta L.,"Flow Field Measurement and Analysis of a 1/7–Scale Mixed Flow Exhaust System Model." AIAA paper 95–2744, July 1995.

2. Castner, R.S., "The Nozzle Acoustic Test Rig; An Acoustic and Aerodynamic Free–Jet Facility." NASA TM 106495, June 1994.

3. Patrick, W.P., and Patterson, R.W., "Seeding Technique for Laser Doppler Velocimetry Measurements in Strongly Accelerated Nozzle Flowfields." AIAA paper 81–1198, June 1981.

4. Wernet, J.H., and Wernet, M.P., "Stabilized Alumina/Ethanol Colloidal Dispersions for Seeding High Temperature Air Flows." NASA TM 106591, June 1994.

5. Ide, Robert F., "Liquid Water Content and Droplet Size Calibration of the the NASA Lewis Icing Research Tunnel," NASA TM 102447, January 1990.

6. Hepner, Timothy E., "State–of–the–Art Laser Doppler Velocimeter Signal Processors: Calibration and Evaluation," AIAA paper 94–0042, January 1994.

7. Edwards, R. V., and Meyers, J. F., "An Overview of Particle Sampling Bias," Second International Symposium on Applications of Laser Anemometry to Fluid Mechanics, , Portugal, 1984.

	Probe Volume Dimensions (mm)			
	On-axis		Off-axis	
	Diam	Length	Diam	Length
Green	0.14	6.9	0.14	1.2
Blue	0.13	6.5	0.13	2.2
Violet	0.16	10.0	0.16	2.4

Table 1. Probe volume dimensions, mm.

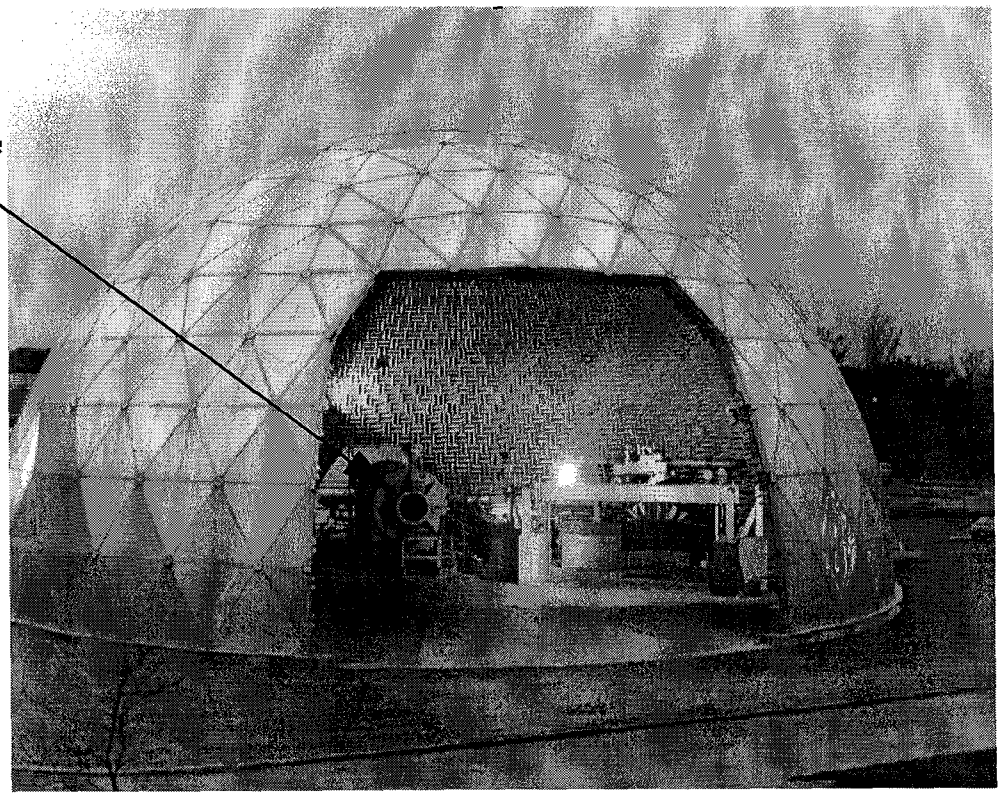

Fig. 1 - Photograph of the Aeroacoustics Propulsion Lab.

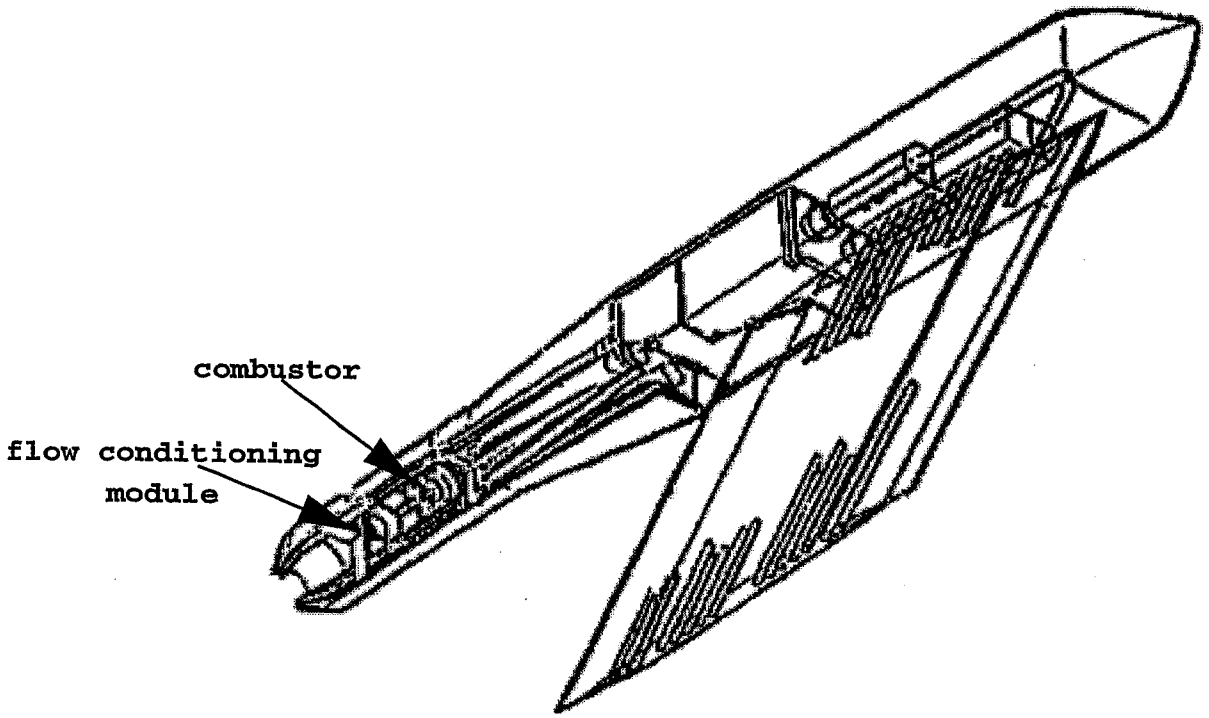

Fig. 2 - Schematic showing strut-mounted Jet Exit Rig.

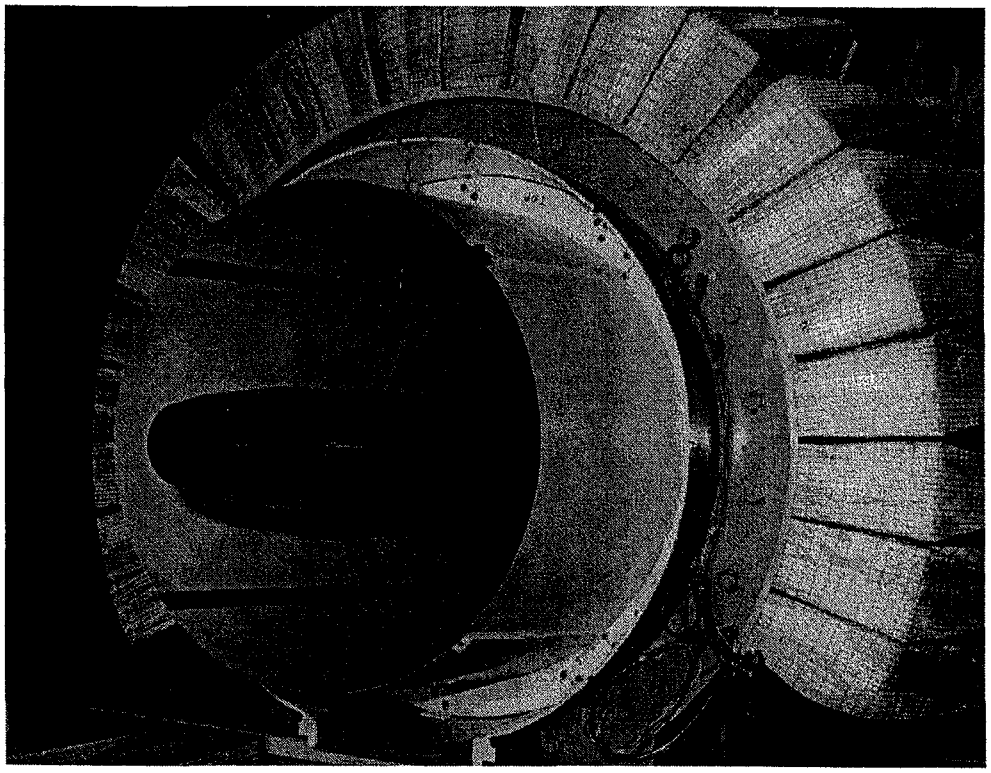

Fig. 3 - Photograph of model installed in NATR.

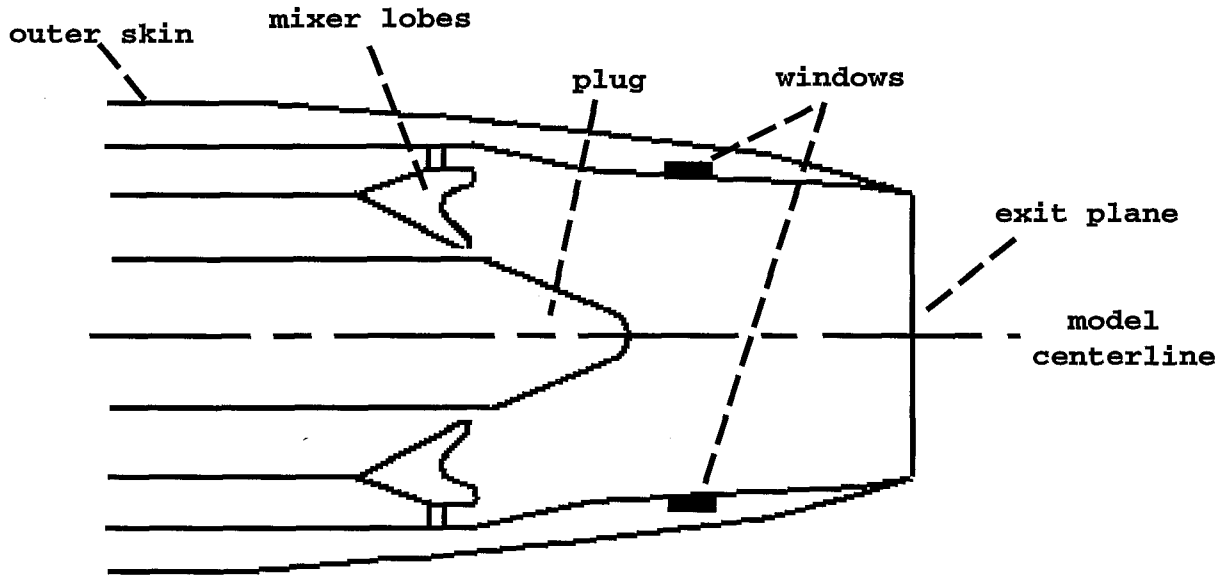

Fig 4. Schematic showing cross-sectional cut through mixer model.

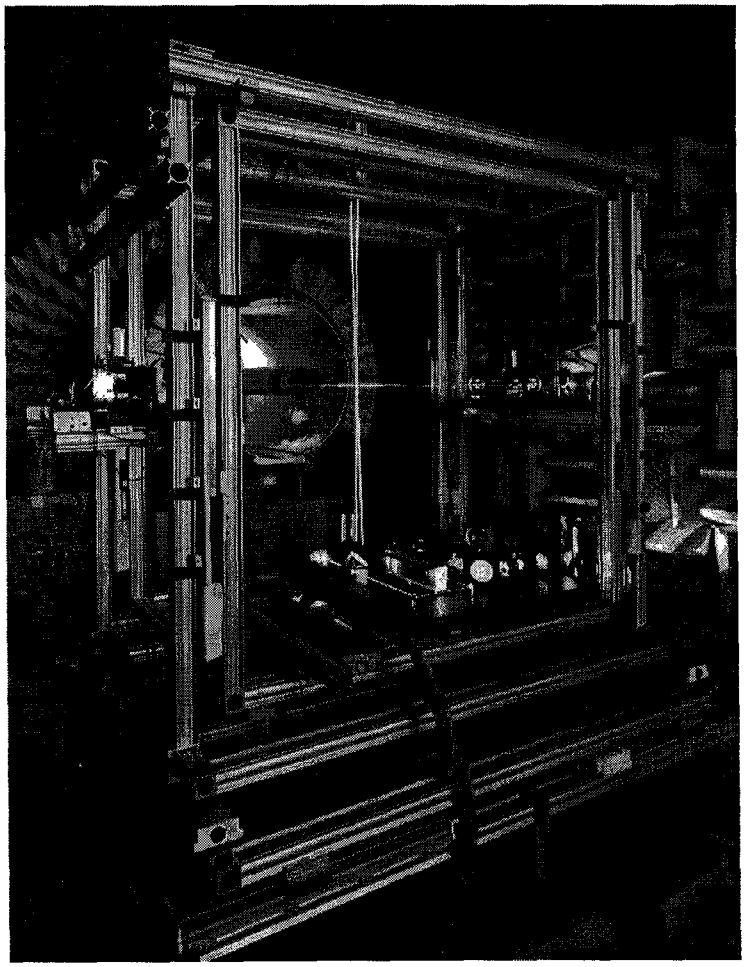

Fig. 5 - Photograph of LDV scan rig.

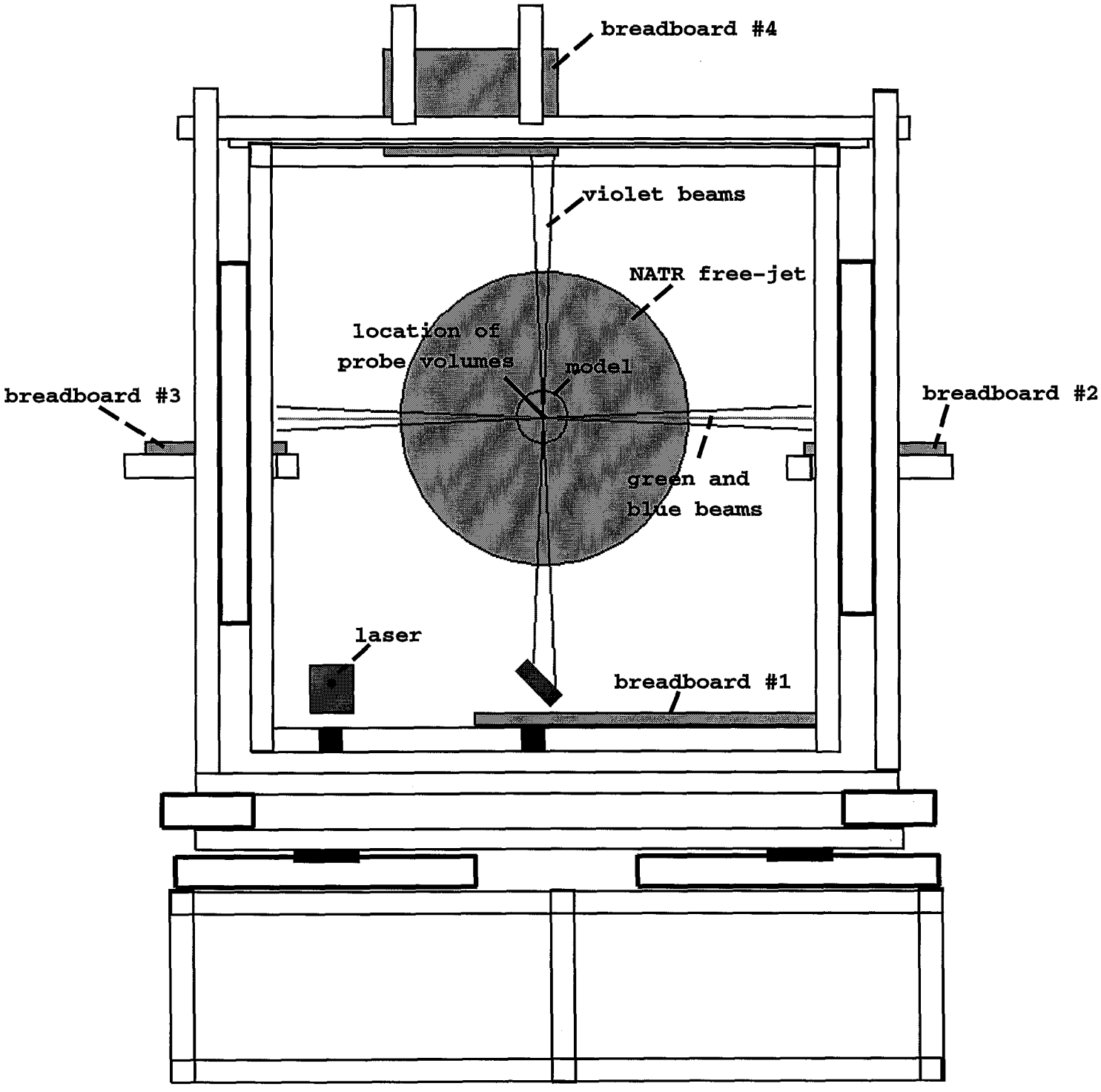

Fig. 6. - Schematic showing optics breadboard locations on LDV scan rig.

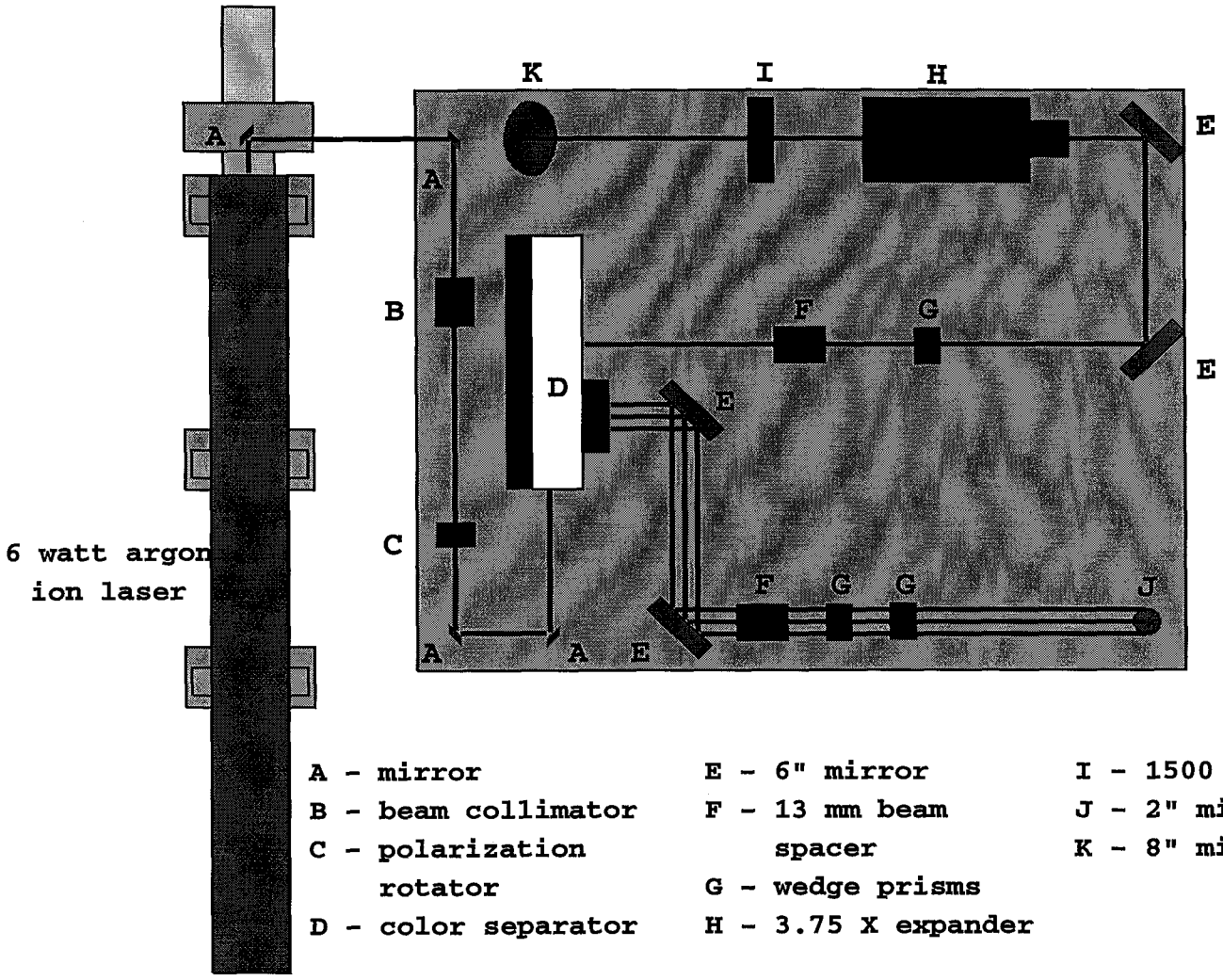

A - mirror
B - beam collimator
C - polarization rotator
D - color separator
E - 6" mirror
F - 13 mm beam spacer
G - wedge prisms
H - 3.75 X expander
I - 1500 mm lens
J - 2" mirror
K - 8" mirror

Fig. 7a - Schematic depicting layout of laser and optics on breadboard #1.

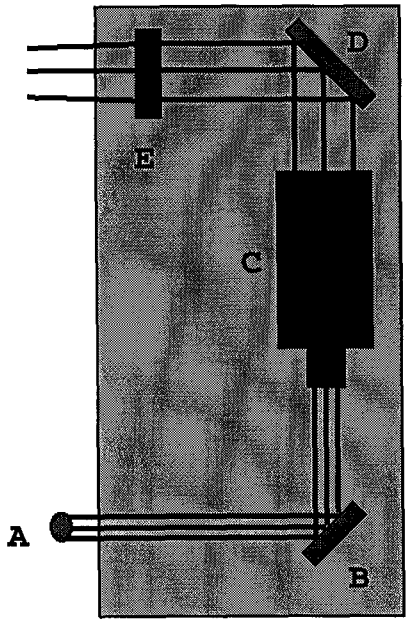

A - 2" mirror
B - 6" mirror
C - 3.75 X expander
D - 8" mirror
E - 1500 mm lens

Fig. 7b - Schematic depicting optics layout on breadboard #2.

A - 1500 mm lens
B - 450 mm lens
C - remotely controlled 6" mirror
D - blue filter, pinhole & photomultiplier tube
E - green filter, pinhole & photomultiplier tube

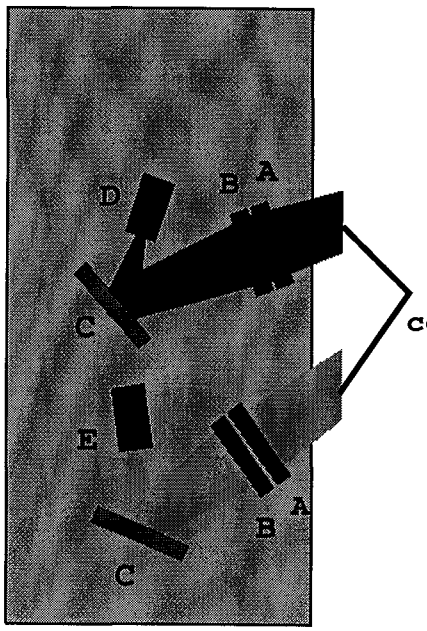

Fig. 7c - Schematic showing optics layout on breadboard #3

A - 1500 mm lens
B - 450 mm lens
C - remotely controlled 6" mirror
D - violet filter, pinhole & photomultiplier tube

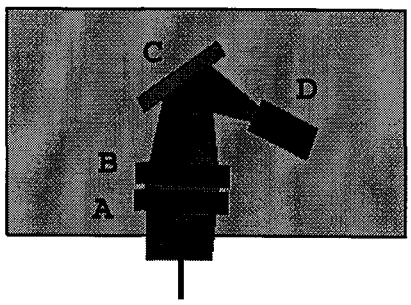

Fig. 7d - Schematic showing optics layout on breadboard #4

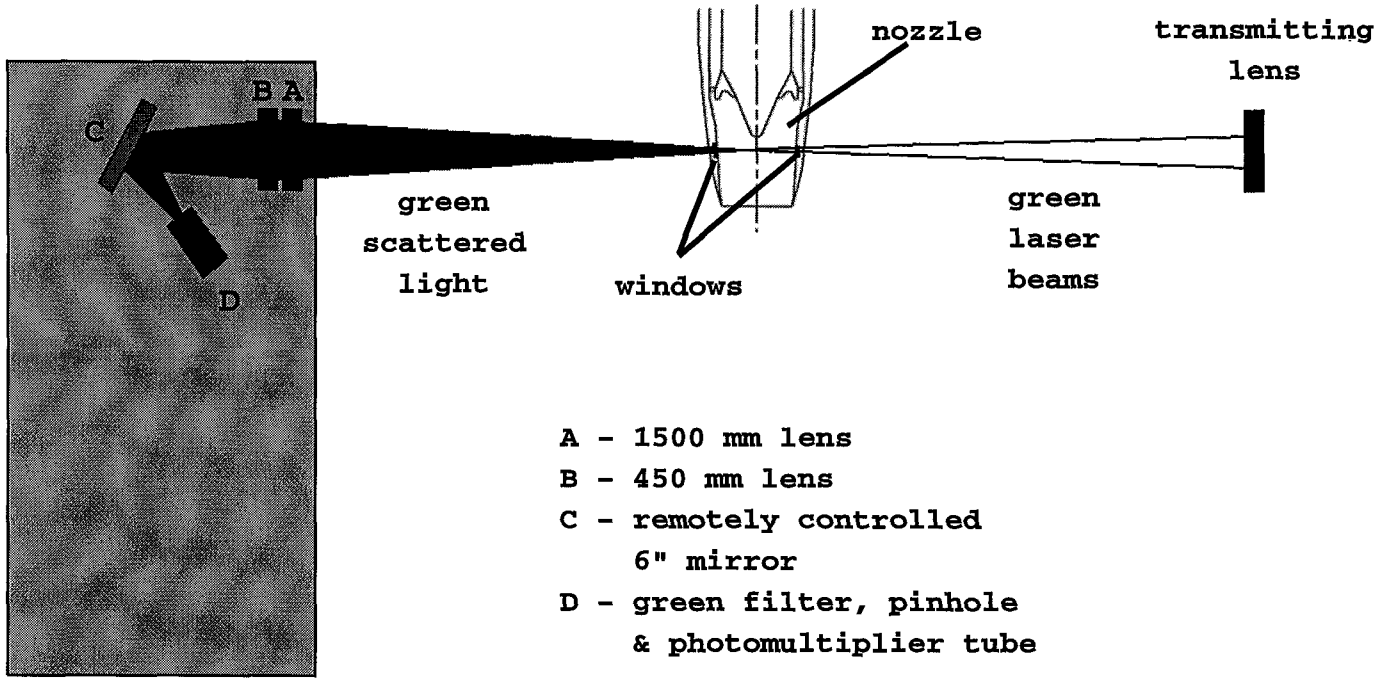

Fig. 8 - On-axis receiving optics configuration for internal flow measurements.

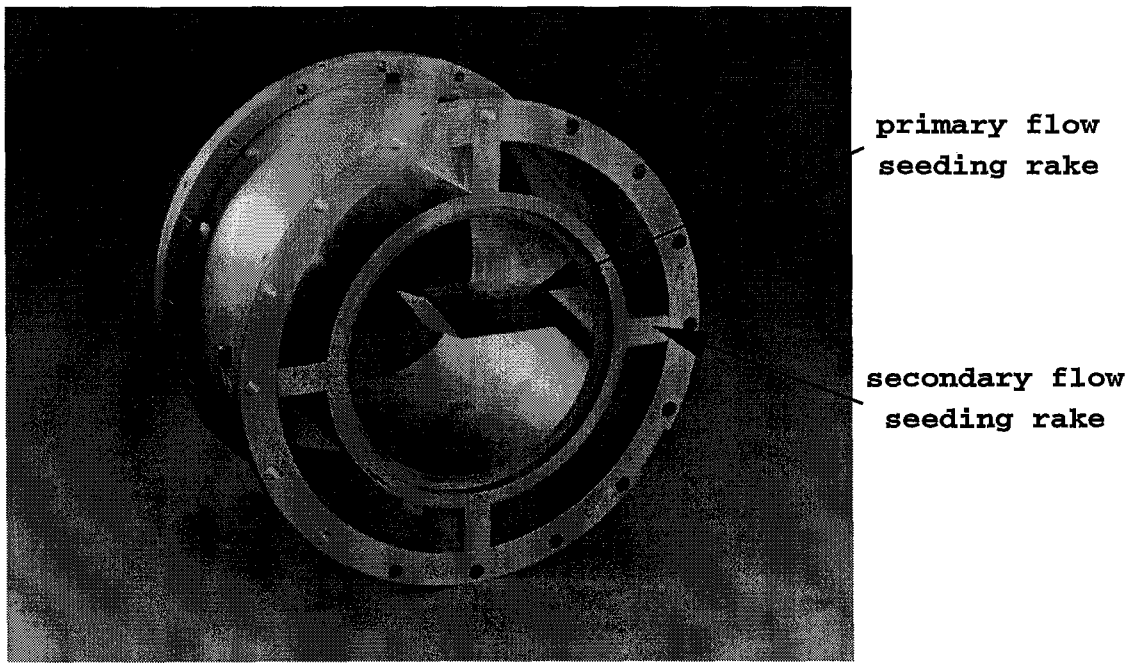

Fig. 9 - Photograph of model spool piece which contains seeding rakes.

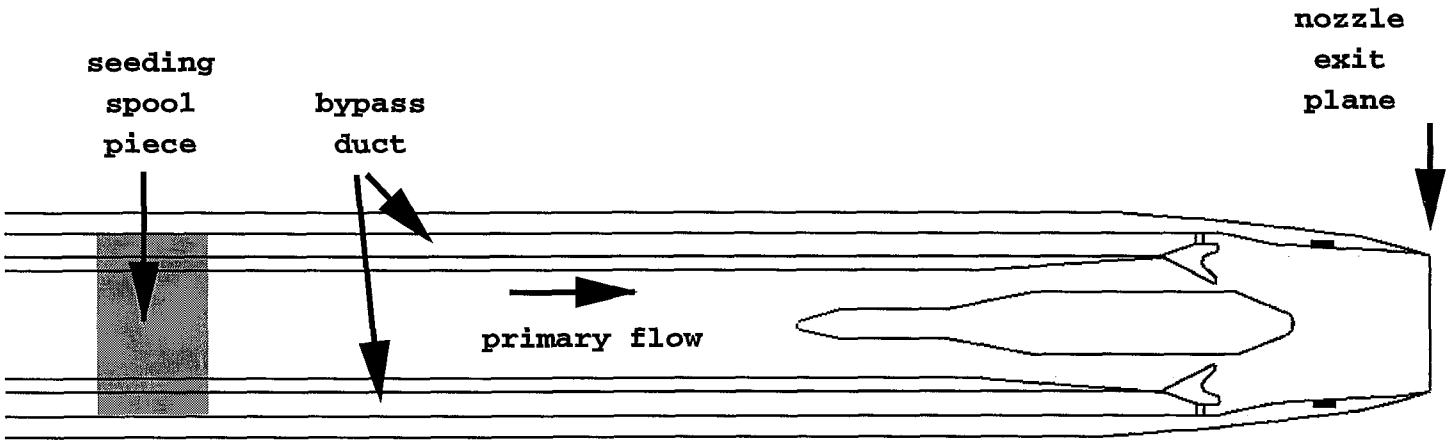

Fig. 10 - Schematic showing location of seeding spool piece within model.

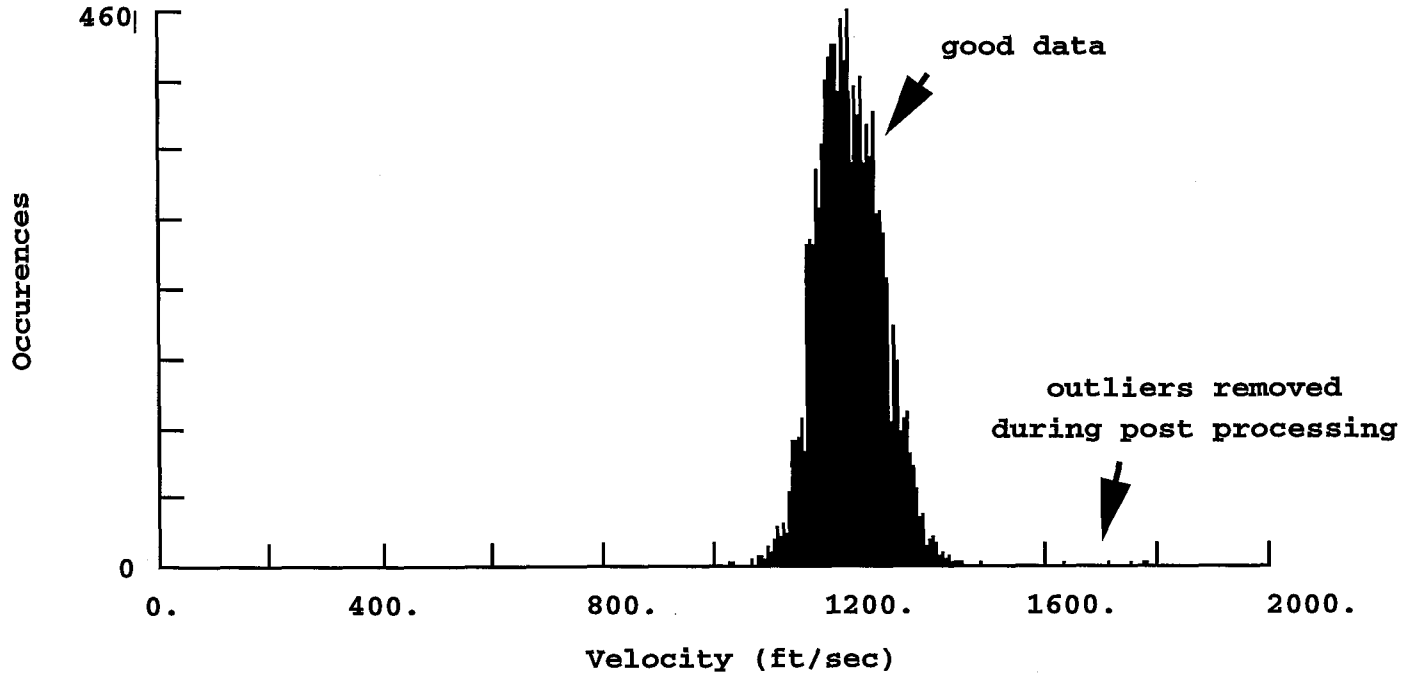

Fig. 11 - Example of velocity histogram showing good data and outliers.

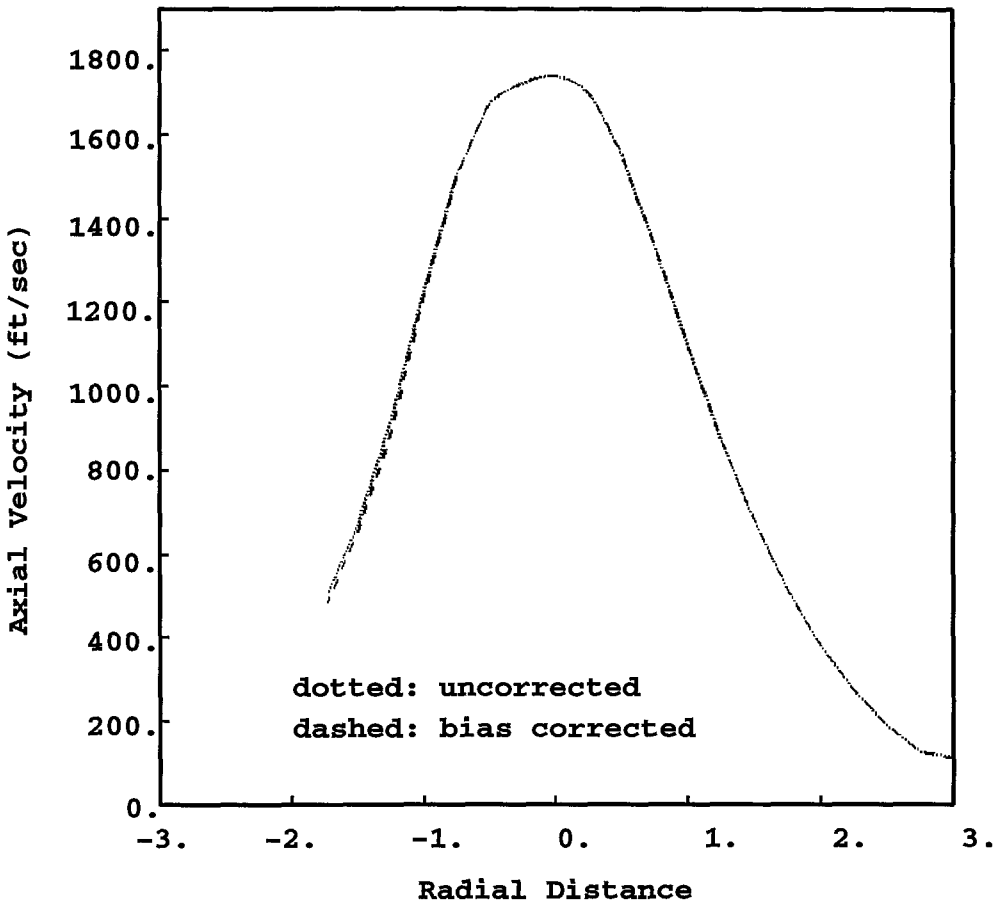

Fig. 12 - Comparison of velocity bias corrected and uncorrected axial velocities. Data shown were obtained in exhaust plume of reference splitter nozzle at x/D=4.

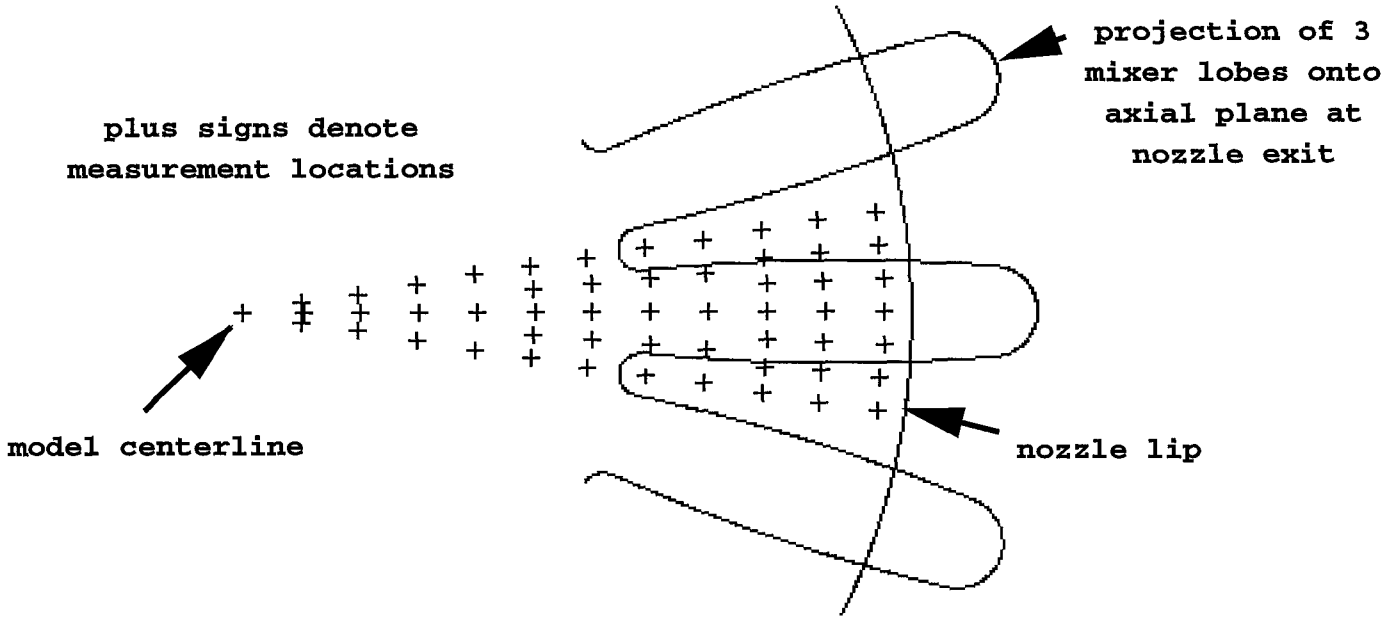

Fig. 13 - Schematic illustrating measurement grid density at nozzle exit measurement location.

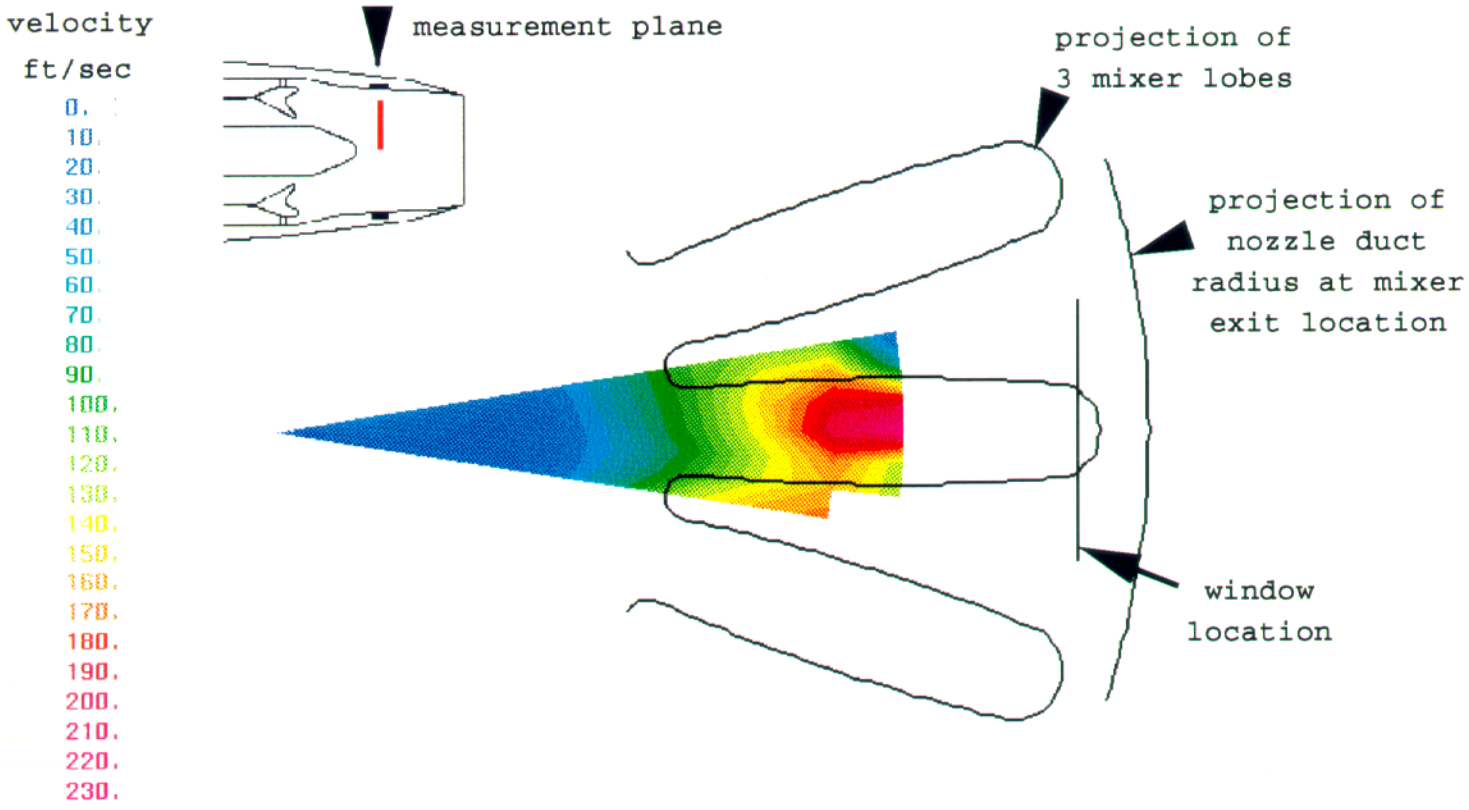

Fig. 14 - Normalized axial velocity contours measured within nozzle tailpipe downstream of 20 lobe mixer. Plotted contours represent the local axial velocity minus the centerline value.

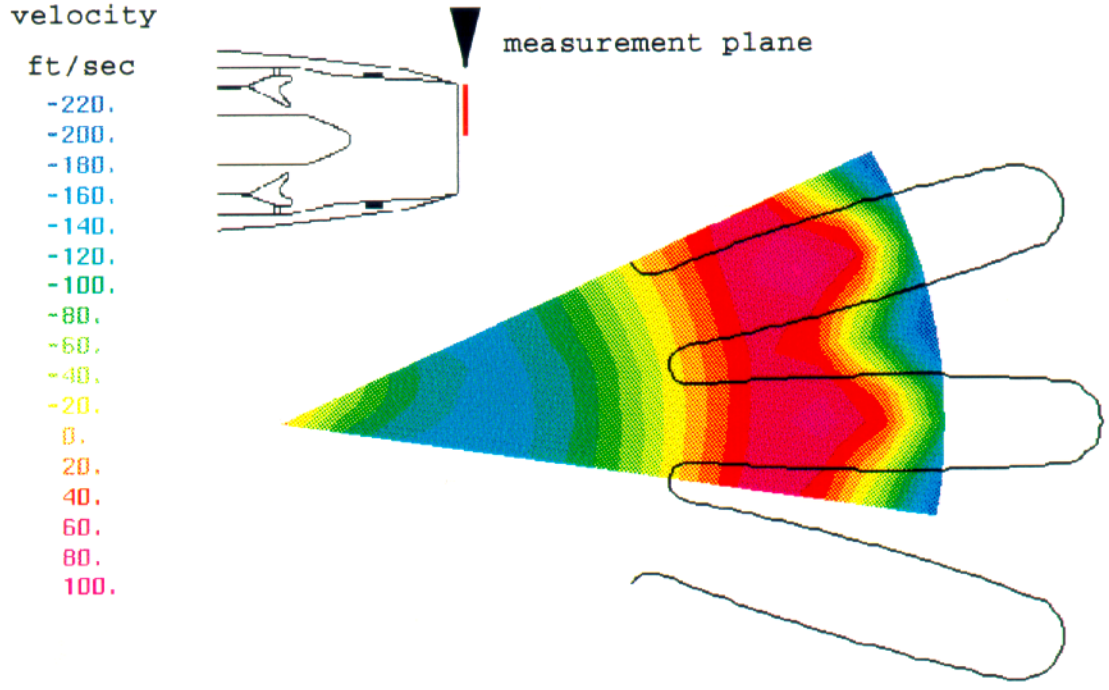

Fig. 15 - Normalized axial velocity contours measured 0.25 inch downstream of nozzle exit with 20 lobe mixer installed. Plotted contours represent the local axial velocity minus the centerline value.

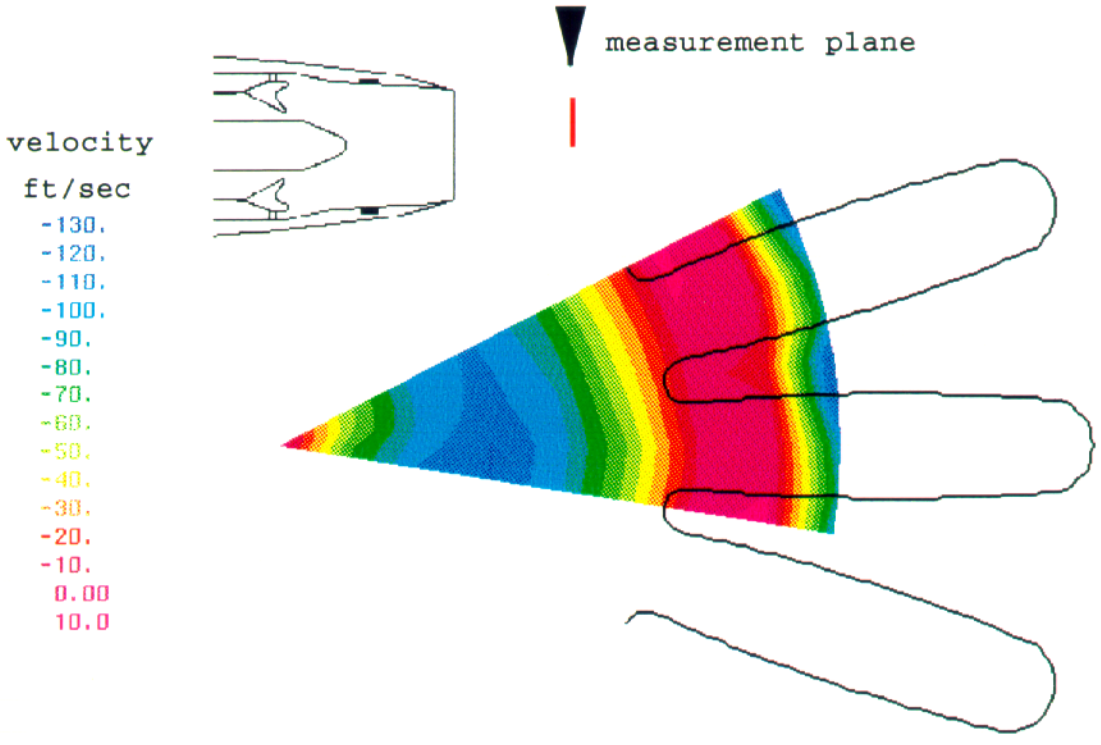

Fig. 16 - Normalized axial velocity contours measured one nozzle diameter downstream of nozzle exit. Plotted contours represent the local axial velocity minus the centerline value.

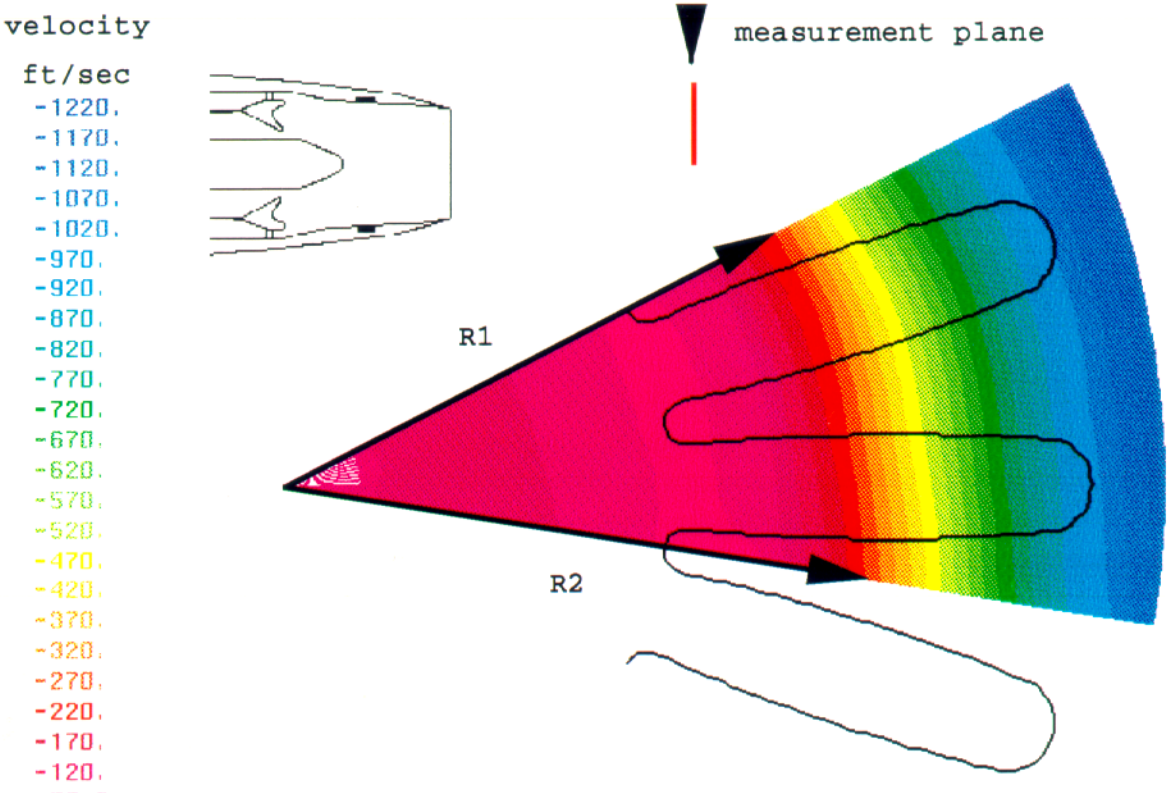

Fig. 17 - Normalized axial velocity contours measured two nozzle diameters downstream of nozzle exit. Plotted contours represent the local axial velocity minus the centerline value.

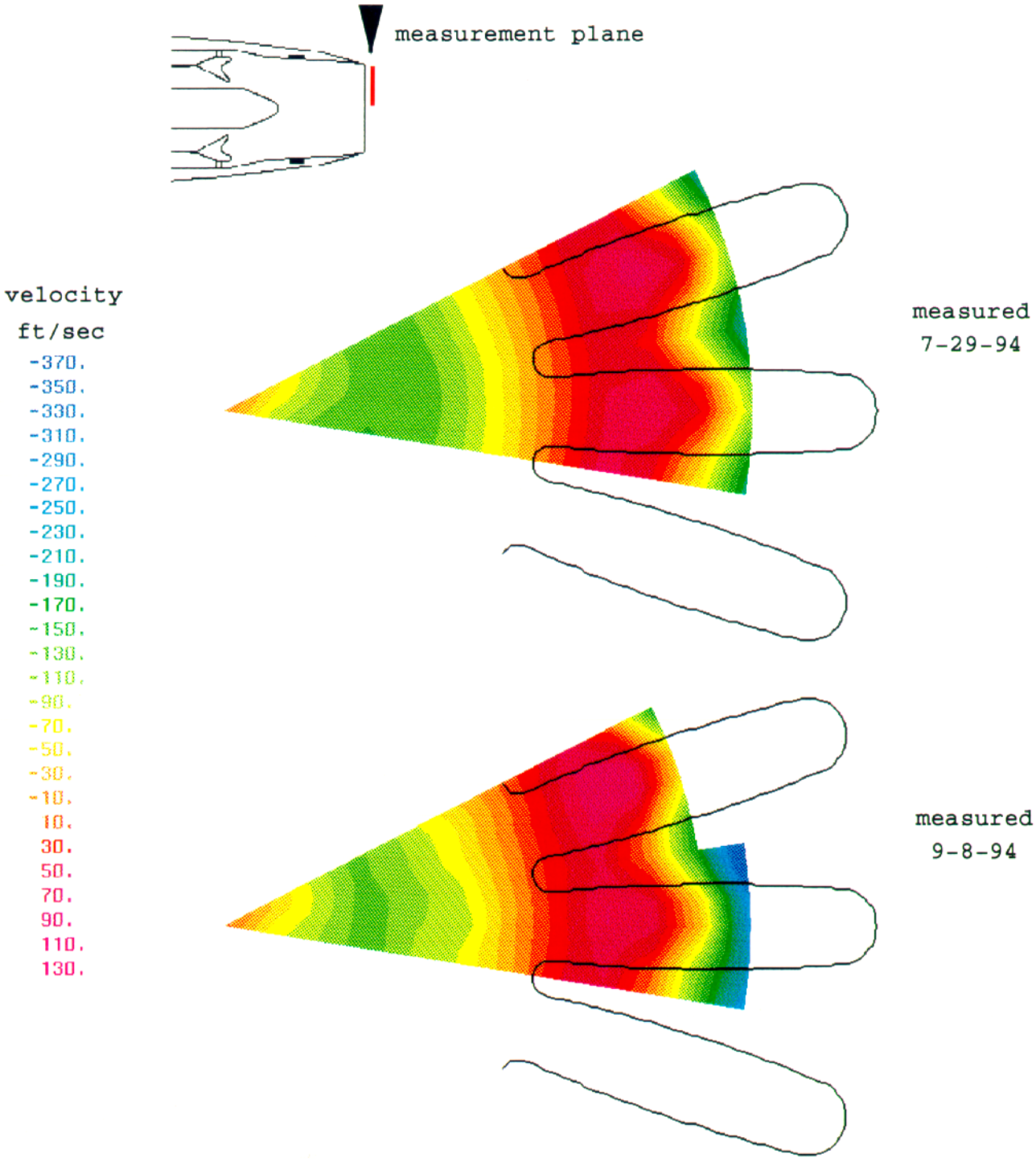

Fig. 18 - Illustration of day-to-day repeatability of data. Plotted contours represent the measured axial velocities minus the centerline axial velocity.

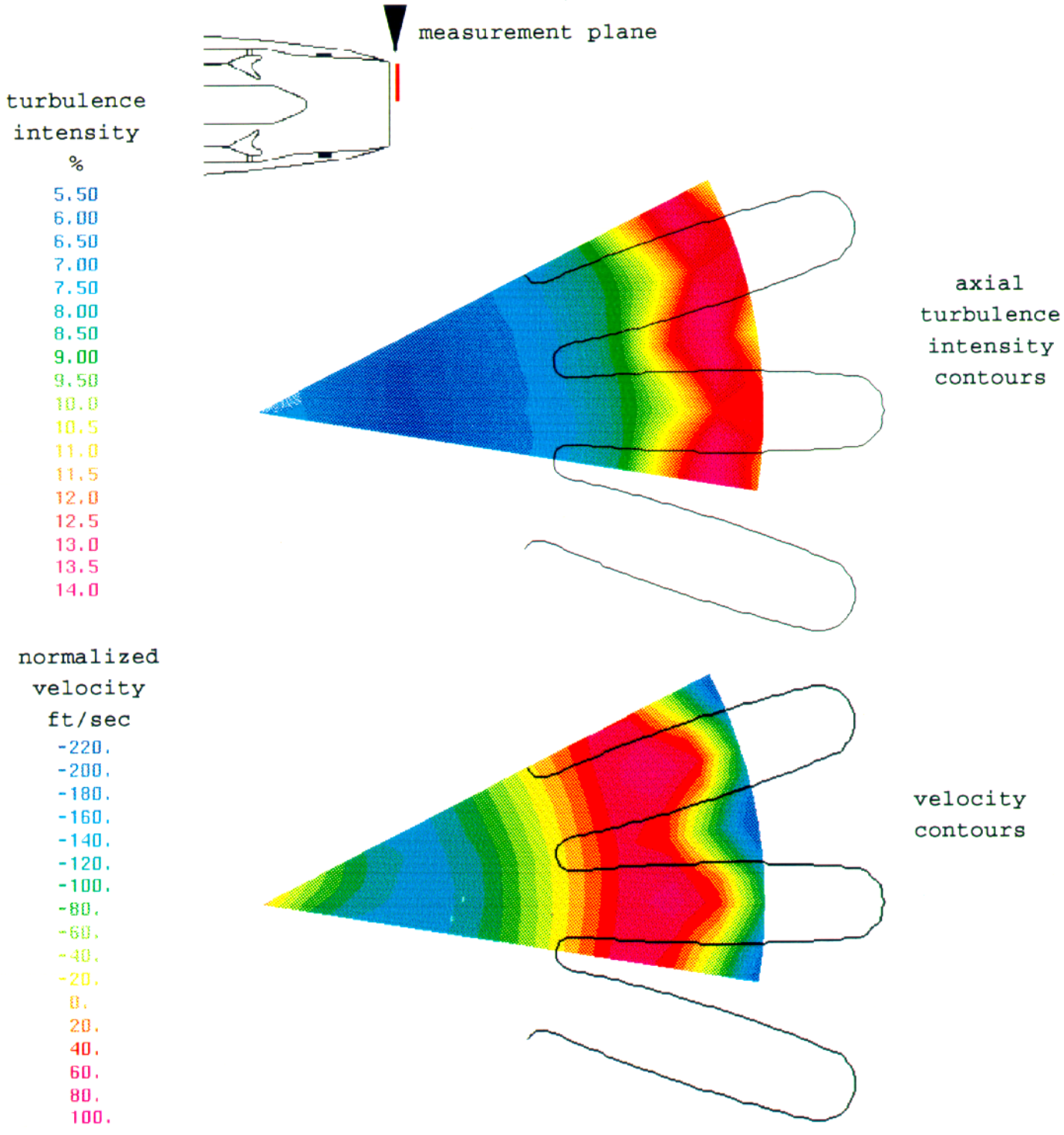

Fig. 19 - Axial component of turbulence intensity contours (top) and normalized axial velocity contours (bottom).

REPORT DOCUMENTATION PAGE

Form Approved
OMB No. 0704-0188

1. AGENCY USE ONLY (*Leave blank*)	2. REPORT DATE	3. REPORT TYPE AND DATES COVERED
	June 1995	Technical Memorandum

4. TITLE AND SUBTITLE

Laser Doppler Velocimeter System for Subsonic Jet Mixer Nozzle Testing at the NASA Lewis Aeroacoustic Propulsion Lab

5. FUNDING NUMBERS

WU–538–03–11–00

6. AUTHOR(S)

Gary G. Podboy, James E. Bridges, Naseem H. Saiyed, and Martin J. Krupar

7. PERFORMING ORGANIZATION NAME(S) AND ADDRESS(ES)

National Aeronautics and Space Administration
Lewis Research Center
Cleveland, Ohio 44135–3191

8. PERFORMING ORGANIZATION REPORT NUMBER

E–9753

9. SPONSORING/MONITORING AGENCY NAME(S) AND ADDRESS(ES)

National Aeronautics and Space Administration
Washington, DC 20546–0001

10. SPONSORING/MONITORING AGENCY REPORT NUMBER

NASA TM–106984
AIAA–95–2787

11. SUPPLEMENTARY NOTES

Prepared for the 31st Joint Propulsion Conference and Exhibit cosponsored by AIAA, ASME, SAE, and ASEE, July 10–12, 1995, San Diego, California. Gary G. Podboy, Naseem H. Saiyed, and Martin J. Krupar, NASA Lewis Research Center; James E. Bridges, NYMA, Inc., 2001 Aerospace Parkway, Brook Park, Ohio 44142 (work funded by NASA Contract NAS3–27186). Responsible person, Gary G. Podboy, organization code 2770, 216–433–3916.

12a. DISTRIBUTION/AVAILABILITY STATEMENT

Unclassified - Unlimited
Subject Categories: 01

Available electronically at http://gltrs.grc.nasa.gov/GLTRS

This publication is available from the NASA Center for AeroSpace Information, 301–621–0390.

12b. DISTRIBUTION CODE

13. ABSTRACT ***(Maximum 200 words)***

A laser Doppler velocimeter (LDV) system developed for the Aeroacoustic Propulsion Laboratory (APL) at the NASA Lewis Research Center is described. This system was developed to acquire detailed flow field data which could be used to quantify the effectiveness of internal exhaust gas mixers (IEGMs) and to verify and calibrate computational codes. The LDV was used as an orthogonal, three component system to measure the flow field downstream of the exit of a series of IEGMs and a reference axisymmetric splitter configuration. The LDV system was also used as a one component system to measure the internal axial flow within the nozzle tailpipe downstream of the mixers. These IEGMs were designed for low-bypass ratio turbofan engines. The data were obtained at a simulated low flight speed, high-power operating condition. The optical, seeding, and data acquisition systems of the LDV are described in detail. Sample flow field measurements are provided to illustrate the capabilities of the system at the time of this test, which represented the first use of LDV at the APL. A discussion of planned improvements to the LDV is also included.

14. SUBJECT TERMS	15. NUMBER OF PAGES
LDV; Mixer nozzles; Exhaust flow	30
	16. PRICE CODE: A03

17. SECURITY CLASSIFICATION OF REPORT	18. SECURITY CLASSIFICATION OF THIS PAGE	19. SECURITY CLASSIFICATION OF ABSTRACT	20. LIMITATION OF ABSTRACT
Unclassified	Unclassified	Unclassified	